Thesis for the degree of Doctor of Philosophy

Dissolution of cellulose in aqueous hydroxide base solvents

BEATRICE SWENSSON

Department of Chemistry and Chemical Engineering
Chalmers University of Technology
Göteborg, Sweden 2022

Dissolution of cellulose in aqueous hydroxide base solvents

BEATRICE SWENSSON

ISBN 978-91-7905-628-5
Doktorsavhandlingar vid Chalmers tekniska högskola.
Ny serie nr 5094 (ISSN 0346-718X).

Department of Chemistry and Chemical Engineering
Chalmers University of Technology
SE-412 96 Gothenburg
Sweden
Telephone +46 (0)31 772 1000

Cover: Illustration by Elin Malmgren, depicting an Erlenmeyer flask containing dissolved cellulose. In the background the X-ray trace of cellulose I and cellulose II can be seen.

Printed by Chalmers Digitaltryck, Göteborg, Sweden 2022

Dissolution of cellulose in aqueous hydroxide base solvents

BEATRICE SWENSSON

Department of Chemistry and Chemical Engineering
Chalmers University of Technology

Abstract
As we move towards a circular bio-economy, new and advanced materials based on cellulose are constantly being developed. Unlike most plastics or metals, cellulose cannot be melted, therefore dissolution is an important tool for both the processing of cellulose and also for analytical purposes. There is, however, both a knowledge gap regarding the understanding of the mechanisms behind dissolution, as well as a continued search for new and improved solvents.

Aqueous solutions of hydroxide bases are a group of solvents with considerable variation in both dissolution capacity and stability of cellulose solutions. Therefore their properties need to be improved in order to be useful solvents. Despite this, they are interesting because they have the potential to be low-cost and non-toxic, depending on the base of choice. Therefore, the purpose of this thesis has been to further understand the interactions governing cellulose dissolution and properties in aqueous solutions of hydroxide bases, so that in the future, new and improved solvents can be designed. In order to achieve this, cellulose dissolution at low temperatures in aqueous solutions of NaOH and selected quaternary ammonium hydroxide bases has been investigated. The effect of combining NaOH with a quaternary ammonium hydroxide was also investigated, along with the influence of the commonly used additive urea.

Results based on light scattering measurements revealed that dissolution in NaOH(aq) is poor, with relatively large aggregates detected already at very dilute concentrations and a fraction of undissolved cellulose always present. Upon comparing NaOH to more hydrophobic quaternary ammonium hydroxides, it was observed that the dissolution capacity of the bases increased with increasing hydrophobicity of the cation, alongside their ability to act as hydrogen bond acceptors. Rheology measurements showed that compared to pure NaOH(aq) or pure tetramethylammonium hydroxide (TMAH)(aq), combining NaOH with TMAH improved the stability of the solutions over time and against increasing temperature. It was therefore proved that combining bases can have a similar effect as introducing an additive, however the results were highly dependent on the base pair employed and indicated that both bases need to be able to dissolve cellulose on their own, within the same temperature interval and be miscible with each other in order to improve solution properties.

Keywords: cellulose; dissolution; solvent; aqueous; NaOH; quaternary ammonium hydroxide

List of publications and presentations

This thesis is based on the following papers:

Paper I: **Dissolution of cellulose using a combination of hydroxide bases in aqueous solution**
Beatrice Swensson, Anette Larsson, Merima Hasani
Cellulose, 2020, Volume 27, pages 101-112.

Paper II: **Probing interactions in combined hydroxide base solvents for improving dissolution of cellulose**
Beatrice Swensson, Anette Larsson, Merima Hasani
Polymers, 2020, Volume 12, Article no. 1310.

Paper III: **Scattering studies of the size and structure of cellulose dissolved in aqueous hydroxide base solvents**
Beatrice Swensson, Anette Larsson, Merima Hasani
Carbohydrate Polymers, 2021, Volume 274, Article no. 118634.

Paper IV: **Time and temperature dependency of cellulose dissolved in combined hydroxide base solvents**
Beatrice Swensson, Alexander Idström, Anette Larsson, Merima Hasani
Submitted manuscript.

Additional publication not included in the thesis:
Aqueous N,N-dimethylmorpholinium hydroxide as a novel solvent for cellulose
Shirin Naserifar, Beatrice Swensson, Diana Bernin, Merima Hasani
European Polymer Journal, 2021, Volume 161, Article no. 110822.

Contribution report

Beatrice Swensson's contribution to the papers presented in this thesis is as follows:

Paper I: Designed and carried out all of the experimental work with the exception of the nuclear magnetic resonance (NMR) experiment, which was performed with the help of the Swedish NMR-centre and interpreted by the main supervisor, Merima Hasani. The results were interpreted, and the article written, together with main-supervisor Merima Hasani and co-supervisor Anette Larsson.

Paper II: Designed and carried out all of the experimental work. Interpreted the results and wrote the article together with Merima Hasani and Anette Larsson.

Paper III: Had the main responsibility for the experimental work and interpretation of the results, but the small angle X-ray scattering experiments were performed together with Sebastian Lages, and static light scattering with Barbara Berke. The article was written together with Merima Hasani and Anette Larsson, and reviewed by Barbara Berke and Sebastian Lages.

Paper IV: Designed and carried out all of the experimental work with the exception of the solid-state NMR, which was performed by Alexander Idström. The results were interpreted, and the article written, together with Merima Hasani, Anette Larsson and Alexander Idström.

Part of the work has been presented by Beatrice Swensson at:

The 15th European Workshop on Lignocellulosics and Pulp (EWLP)
Poster presentation
Aveiro, Portugal, 26-29 June 2018

The Treesearch Progess conference
Oral presentation
Norrköping, Sweden, 8-9 May 2019

The 6th International Polysaccharides Conference arranged by the European Polysaccharide Network of Excellence (EPNOE)
Oral presentation
Aveiro, Portugal, 21-25 October, 2019

The 7th International Polysaccharides Conference arranged by the EPNOE
Oral presentation
Nantes, France, 11-15 October, 2021

Acknowledgments

First I would like to acknowledge that the research in this thesis was mainly funded by FORMAS, the Swedish Research Council for Sustainable Development, and a minor part by VINNOVA, Sweden's innovation agency.

On a more personal note I want to acknowledge my wonderful main supervisor Merima Hasani. I am truly grateful for your guidance as well as the fact that you have encouraged me to contribute with my own ideas and grow into an independent researcher. You once said that you would do everything in your power to make my time as a PhD student as rewarding, challenging and exciting as it can be, and I really feel that you have.

Secondly, I want to acknowledge Anette Larsson, my co-supervisor. I have often said that I am so grateful for you bringing me energy and hope. I always look forward to our meetings because you make sure that we elevate the scientific discussions and look beyond the latest measuring point!

During the past few years it has also become increasingly important that my colleagues at SIKT are ever so important in giving the everyday life meaning, and I am really grateful for the great atmosphere that we have developed! PhD students, postdocs, researchers and supporting staff alike; I am grateful to Malin, Ximena, Anna and Michael for making everything run so smoothly and providing positive encouragement while doing it. I also want to thank my examiner (and boss for most of my time), Hans Theliander for his encouragement and support.

I want to acknowledge my co-authors Sebastian Lages, Barbara Berke and Alexander Idström for nice scientific discussions and cooperation.

Since the road to a PhD is long, I also want to acknowledge Derek Gray for putting me in contact with Merima in the first place, Monica Ek for showing me the chemistry of wood and Helena Lennholm for raising my interest in chemistry!

Last but not least I want to thank my friends and family in Gothenburg and Stockholm alike, for supporting me along the way.

Contents

1 Theory and background

1.1 Introduction to the thesis

Cellulose is one of nature's building blocks as it is the main constituent in the cell wall of plants, making it an abundant and renewable resource. In Sweden today, almost 70 % of the country is covered with forest [1], and the Swedish forest industry is one of the world's largest exporters of pulp and paper [2]. The traditional products commonly produced from cellulosic pulp are various types of paper, cardboard and textile fibres, but also cellulose derivatives such as cellulose esters or ethers [3]. Most of these products are still highly relevant; it is predicted that the growth in the production and sales of paper packaging will continue, possibly due to an increasing world population consuming products. This will also increase our textile consumption and the need for hygiene paper products. On the other hand, the demand for products such as newspapers, have already declined significantly [4]. There are however new products and applications continuously being developed, such as hydro- and aerogels, barrier films and new types of textile fibres. For many of these materials or applications there is a desire to re-shape or derivatise cellulose, however since it degrades before it melts, it cannot be processed in the same way as traditional plastics or metals. Processing can be performed in the form of suspensions, but proper dissolution of cellulose in a solvent is a crucial tool to fully utilise its potential. Dissolution is for example required to derivatise the cellulose under homogeneous reaction conditions and can also be important in regard to analytical methods to determine the molecular weight distribution [5], or for solution spectroscopy for investigating chemical structures and interactions [6].

To meet the demands of the various applications, there is a need for a range of solvents. For one application it might be vital to produce stable solutions without degrading the cellulose, while for another a high dissolution capacity might be more important. It is essential to understand the mechanism and driving forces behind cellulose dissolution in order to develop new solvents and improve dissolution-based processing and applications. This thesis deals with water-based solvents of hydroxide bases, with a special focus on dissolution in aqueous solutions of NaOH and quaternary ammonium hydroxides. These have been known cellulose solvents for almost a century, but they have yet to be utilised on an industrial scale or for analytical purposes. For NaOH(aq), dissolution is quite poor and has to be improved in order to be useful. Despite the long research history there is still a lack in knowledge regarding the mechanisms behind dissolution and how to improve it. Compared to NaOH, the quaternary ammonium hydroxides make better solvents for cellulose but suffer from the same knowledge gap. Despite these drawbacks, there is still a continued interest in these solvents, especially in utilising NaOH, because it is a chemical readily used by the pulp and paper industry, is low-cost and non-toxic.

The overarching purpose of this thesis has therefore been to further improve knowledge on dissolution of cellulose in aqueous solutions of hydroxide bases, and to use this knowledge to develop and improve such water-based solvents, with a special focus on dissolution in NaOH(aq). This has been achieved by a broad investigation of several different hydroxide bases, which also led to the idea that NaOH could be combined with another base to improve solution properties. In order to narrow down the investigation, the focus was selectively put on hydroxide bases that require low temperatures to dissolve cellulose and the following objectives were addressed:

- To improve our understanding of the role of the cation in dissolution and stabilisation of the cellulose.
- To understand which bases can be combined with NaOH and how it can affect dissolution.
- To improve our understanding of the temperature dependency of dissolution in these solvent systems.

1.2 Cellulose

Cellulose is a linear and unbranched polymer consisting of β-1,4-linked D-glucopyranose units. Each cellulose chain has two odd ends: one non-reducing and one reducing end, the latter can ring-open to form an aldehyde (see Figure 1.1). As mentioned, cellulose is mainly found in the cell wall of plants and although there are other sources of cellulose, such as bacteria or tunicates, the main sources are cotton and wood. Cotton is almost pure cellulose, but in wood cellulose co-exists with lignin and hemicellulose. The liberation of cellulose from the wooden matrix has consequences for its structure, such as: reduced chain length, introduction of oxidised groups and changes in the ultrastructure.

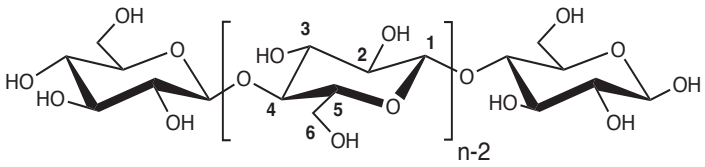

Figure 1.1: The structure of the repeating unit of cellulose, the anhydroglucose unit (AGU) and the non-reducing end group to the left, and the reducing end group to the right.

Native cellulose

The cellulose chains in their native form can reach an average of up to ca. 10 000 repeating units, however they are typically closer to 2000 units after pulping, and there is always a wide distribution of the chain lengths. The crystalline structure of native cellulose is called cellulose I, which consists of a mix of two crystal forms: I_α and I_β, where I_β dominates in cellulose originating from wood [7]. Along the chains of native cellulose there are intramolecular hydrogen bonds between the hydroxyl group on the C6 and the C2', and between the oxygen in the ring and the hydroxyl on the C3 (see

Figure 1.2). The hydroxyl groups in the cellulose glucose units are all arranged in an equatorial position, which also allows them to create an intermolecular network of hydrogen bonds between neighbouring cellulose chains. The chains are arranged parallel to each other, with an intermolecular bond between the hydroxyl on C6 and that of C3" on an adjacent chain, as illustrated in Figure 1.2 [8]. There is no such possibility for traditional hydrogen bonding in the axial direction of the pyranose ring, but the cellulose chains can interact via London dispersion (van der Waals) forces and via unconventional C–H···O hydrogen bonding. Although classical hydrogen bonds are important for the properties of cellulose, it has been shown that it is in fact the London dispersion forces that are the main contributor to the cohesion of the cellulose [9][10].

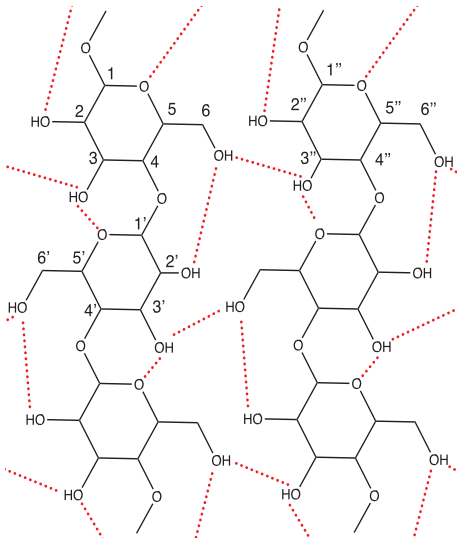

Figure 1.2: Illustration of the hydrogen bonding in and between native cellulose chains, adapted from Henriksson and Lennholm [8].

As most polymers, cellulose is not an entirely crystalline material but in addition to less ordered regions, it also has a complex hierarchical structure. This hierarchical structure differs depending on the plant and the cell type from which the cellulose originates. For cellulose from wood the chains pack into elementary fibrils with a diameter of 3-4 nm, with regions that are more or less disordered and not entirely crystalline. In turn, these fibrils bundle into macrofibrils with a diameter of 10-25 nm. These macrofibrils exist in the cell wall, which has a layered structure, with both a primary and secondary wall outside the lumen, and these walls are surrounded by the middle lamella (see Figure 1.3). The middle lamella is filled with lignin which is removed upon pulping. In the primary wall the macrofibrils have almost no orientation, and the fibrils are arranged randomly, but the secondary wall is divided into different layers with different fibril orientations. With regards to the fibre axis, the fibrils in the first and third layer of the secondary wall are arranged almost horizontally, while in the second layer (the major part of the secondary wall) the orientation is close to vertical [8],[11].

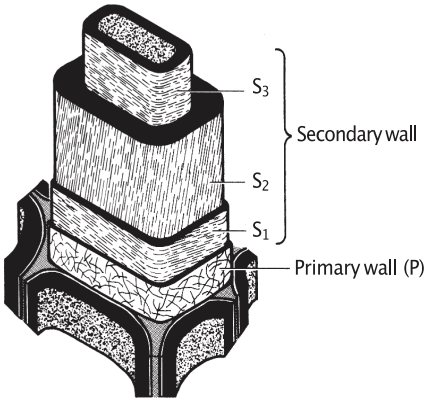

Figure 1.3: Illustration of the layers of the cell wall, adapted from Schmulsky and Jones [12], with permission from the publisher.

Cellulose II

There are several other crystal structures which cellulose can adapt besides cellulose I, the most common being the cellulose II structure, where the chains are arranged anti-parallel to each other. Cellulose can be converted from cellulose I into cellulose II through various treatments, the most notable ones being through dissolution and regeneration/coagulation, or by immersing it in NaOH(aq) without dissolution (called mercerisation) [13]. There are other treatments reported, for example acid hydrolysis [14], or ball milling when wet [15], the commonality being that they induce intracrystalline swelling. The transformation from cellulose I to cellulose II is however irreversible, and has been attributed to the cellulose II crystalline form being thermodynamically more stable. In cellulose II the intramolecular hydrogen bond between the oxygen in the ring and the C3' hydroxyl remains, but that between the C6 and the C2' hydroxyl groups has not been formed. This most likely contributes to the significant reduction in elastic modulus compared to cellulose I [16]. There are however, several possibilities for intermolecular bonding in cellulose II, and the reader is referred to Langan et al. for a detailed description [17].

1.3 Dissolution of polymers

In order for a polymer to dissolve in a given solvent the Gibbs free energy change upon mixing must be negative [18]. This depends on both the entropic and enthalpic contributions as seen in Equation 1.1. The enthalpic contribution is determined by the the bonds and interactions between the molecules in solution. The interactions between cellulose (the solute) and the solvent needs to overcome the attractive interactions between the cellulose chains as well as the solvent-to-solvent interactions. The entropic contribution is determined by the difference in entropy upon dissolution. For strong polyelectrolytes, polymers with groups that completely ionize in solution, it is recognized that entropy plays a significant role in their strong swelling at low salt concentrations, due to an entropy gain upon the release of counterions.

This effect is less dominant for weak polyelectrolytes [19]. For cellulose, the entropic contribution will, for example, be affected by the chain length: with decreasing chain length the entropy gain will increase, and therefore it is easier to dissolve shorter cellulose chains. Another reason for the favouring of dissolution is the conformational freedom that a polymer can gain upon dissolution, which will be higher for flexible polymers but lower for semi-stiff polymers such as cellulose.

$$\Delta G_m = \Delta H_m - T\Delta S_m \tag{1.1}$$

An ideal and flexible polymer in a good solvent will adapt a so-called Gaussian chain, where the conformations of the segments are randomly distributed [18]. The opposite to a fully flexible Gaussian chain is a stiff rod-like cylinder. Cellulose, being a semi-stiff polymer, would most likely assume a conformation somewhere between these two. For semi-stiff polymers, the model of a so-called worm-like chain can be used. The theoretical radius of gyration for a polymer can be calculated from these models, and the equation for the model of a Gaussian coil is given in Equation 1.2 [20], the equation for a rigid rod (cylinder) in Equation 1.3 [20], and the equation for a worm-like chain in Equation 1.4 [21].

$$R_g = \sqrt{\frac{Nb^2}{6}} \tag{1.2}$$

Where N is the number of Kuhn monomers of length b [20].

$$R_g = \sqrt{\frac{d^2}{8} + \frac{L^2}{12}} \tag{1.3}$$

Where d is the diameter of a cylinder of length L [20].

$$R_g = \sqrt{\frac{Ll_p}{3} - \frac{{l_p}^2}{3}(1 - exp(-L/l_p))} \tag{1.4}$$

Where l_p is the persistence length and L the contour length [21].

In general dissolution of polymers differ from dissolution of low molecular weight compounds due to the two-step process. For 'normal polymer dissolution' the solvent first needs to diffuse into the polymer, creating a gel-like swollen layer with two interfaces: one between the solvent and the gel, and another between the gel and the solid polymer. Secondly, the chains need to disentangle and disperse in the solvent [22]. Because of this, the chain length also influences the dissolution rate, which decreases with increased molecular weight, as large molecular weights yield higher levels of entanglement. In general, the dissolution rate can be increased by stirring because the gel layer is carried off by the solvent. The importance of the chain disentanglement has been shown for cellulose through an experiment where the cellulose fibres were placed under tension, reducing the swelling and dissolution capacity due to the inhibited movement of the chains [23].

1.4 Solubility of cellulose

Cellulose is insoluble in water (despite the ample opportunity for hydrogen bonding) and also in common organic solvents. In water, the insolubility has been discussed in terms of a hydrophobic effect due to the amphiphilic character of cellulose [24]. It can be described as following: there is a strong network of hydrogen bonds between water molecules in bulk, this is broken around the less polar (more hydrophobic) pyranose ring in the axial direction as it cannot participate in traditional hydrogen bonding. The water molecules situated in this area might suffer both from fewer hydrogen bonds (enthalpic punishment) and be more restricted in their mobility (entropic punishment), leading to favourable interactions if the cellulose chains stack and exclude water from the hydrophobic surface. As such, it is debated if the hydrophobic (assembly) effect is driven mainly by a change in enthalpy or entropy [25].

One thing to keep in mind is that cellulose can be extracted from many different sources and also by many different processes, which will lead to a wide range of celluloses with different solubility. Factors such as the molecular weight, molecular weight distribution, purity, crystal structure and crystallinity can affect the solubility, or at least the dissolution rate. Different pretreatments can affect how much of the native structure of the cell wall that remains, and this is also very crucial for dissolution. Moigne at al. have shown that the microstructure and chemical environment of the chains can be more limiting than the chain length [26]. An example of this is the phenomena of ballooning that can occur for cellulose where the primary cell wall remains. The cellulose in the S2 layer of the secondary cell wall dissolves, surrounded by a membrane of swollen S1 layer, with sections of undissolved primary wall in between the 'balloons' (see Figure 1.4) [27][28].

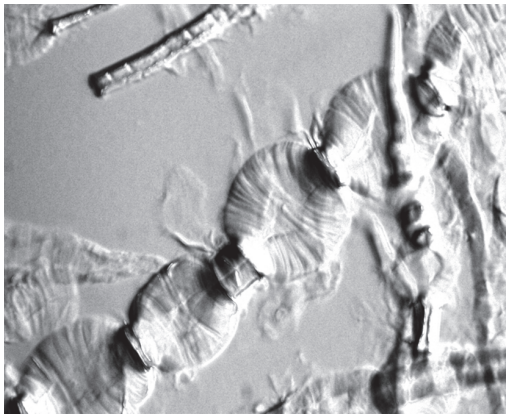

Figure 1.4: Dissolving pulp swollen and partially dissolved in 2 M NaOH(aq) at - 5 °C.

It is also important to stress that since it is a highly polydisperse polymer, the meaning of solubility and the maximum concentration that can be dissolved can be two different things. It is not so that the cellulose will be moleculary dissolved, and then upon addition of more cellulose a classical saturation point will be reached. The solubility of a given cellulose may never reach 100 %, but still the total dissolved amount can increase if more cellulose is added, as recognized already in 1934 by Davidson [29].

1.5 Solvents for cellulose

Before moving on to describe the solvents that can directly dissolve cellulose, it should be mentioned that the most common way to dissolve it is by derivatising cellulose into a more easily soluble cellulose derivative, which after dissolution, is regenerated back into cellulose by cleaving off the attached side groups. This approach often requires more process steps than direct dissolution. The main industrial process where cellulose is dissolved is based on a derivatising approach called the Viscose process, and it has been in operation since the start of the 20^{th} century. It involves several steps, where the cellulose is immersed in a NaOH(aq) solution and reacted with carbon disulfide into cellulose xanthate, which dissolves in NaOH(aq) and forms a so-called dope. This dope is then spun into an acid bath containing sulphuric acid, regenerating the cellulose. While modern processes recover the carbon disulfide, NaOH and sulphuric acid are spent and large amounts of Na_2SO_4 are produced as a by-product [30]. There are still derivatising approaches being proposed for dissolution on an industrial scale, such as the carbamate process where cellulose is reacted with urea at elevated temperatures and pressure, but it has not reached industrial applications so far [31].

There are today a number of solvents that are known to be able to directly dissolve cellulose, and starting from the early 2000s, there has been an increase in the number of research articles on dissolution of cellulose (see Figure 1.5). A few examples of direct solvents are ionic liquids (BMIMCl [32][33], EMIMAc[34]), DMAc/LiCl[35], N-methylmorpholine-N-oxid(NMMO) [36], DMSO/TBAF[37] and NaOH/urea(aq)[38]. The only one which is used on an industrial scale is NMMO, in the form of a monohydrate. It is used for producing man-made cellulosic textile fibres, so-called Lyocell fibres [39]. Advantages with NMMO as a solvent are that it is biodegradable, non-toxic both for human health and ecosystems and can be recycled to 99 %. It is however also a strong oxidant and therefore stabilizers are required to eliminate the risk of runaway reactions and explosions [40]. The focus of this thesis is on investigating cellulose solutions in direct and water-based hydroxide solvents, and they will be described in more detail in the following sections.

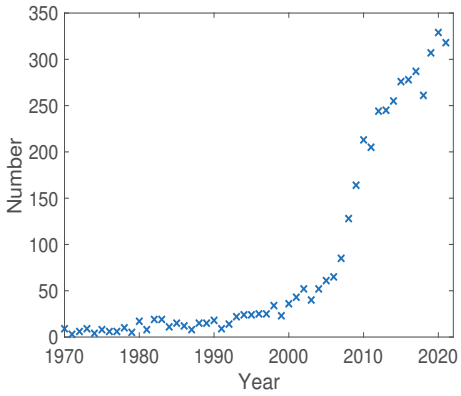

Figure 1.5: Number of articles published per year, indexed in Scopus, related to dissolution of cellulose (when searching for "cellulose and dissolution", excluding articles on pharma).

Aqueous solutions of hydroxide bases as direct solvents for cellulose

There are several hydroxide bases that can dissolve cellulose in aqueous solution: the alkali bases sodium hydroxide (NaOH) and lithium hydroxide (LiOH) [28] [41], and different quaternary ammonium and phosphonium hydroxides [42]. As can be observed, they all carry the same hydroxide anion, which is the strongest base that exists in water. If the cation of the quaternary ammonium hydroxides is instead paired with another suitable anion, it can also be used to dissolve cellulose in solvents other than water. For example, tetrabutylammonium hydroxide (TBAH) can dissolve cellulose in water [43], while tetrabutylammonium fluoride (TBAF) [37] and tetrabutylammonium acetate (TBAAc) can dissolve cellulose in DMSO [44]. From this it can be deduced that the anion plays an important role in the dissolution of cellulose in hydroxide base solvents.

The alkali bases

The discovery that aqueous solutions of sodium hydroxide at low temperatures (usually below zero) can dissolve cellulose was made as early as the 1920s, as can be seen in a patent by Lilienfeld [45]. Further research on the subject was conducted in the 1930s and it was suggested by Davidson that in NaOH(aq), cellulose acts as a very weak acid and forms a salt with the NaOH, 'sodium cellulosate,' which is soluble in alkali [29]. Much of the findings from this early research still hold, such as the observation that there is one maximum for solubility that increases with decreasing temperature and also occurs at lower alkali concentrations [41]. In these early works, Sobue et al. made a phase diagram of the crystalline structures of ramie fibres using X-ray diffraction. They observed that, within a narrow concentration interval of 7 - 8 wt% NaOH(aq), at -5 °C to +1°C, the fibre swelled extraordinarily and became transparent. At low temperatures, below 7 - 8 wt% NaOH(aq), the structure of cellulose I was maintained. Above this concentration, different structures denoted Na-Cell I or Na-Cell V were observed [46]. This is important because it illustrates that there is both a lower and an upper limit to the NaOH concentration where dissolution occurs. This limit has in literature been discussed in terms of the size of the hydrated NaOH [28][47]. The lower limit is perhaps more intuitive than the upper limit, as pure water does not dissolve cellulose. If the cellulose is considered a weak acid that becomes partly deprotonated, it can be viewed in terms of reaching the pKa concentration. The deprotonation of cellulose and the relevance of this for dissolution of cellulose in NaOH(aq) and other solutions of hydroxide bases, is however uncertain. Some authors stress its importance [48], while some do not discuss deprotonation, but only hydrogen bonding between the hydroxide anion and the hydroxyl groups of cellulose. It is notable that it is difficult to detect and quantify deprotonation in this system due to the high concentration of base. There are a few studies trying to model or measure this: Isogai studied a model substrate for cellulose in NaOD/D_2O with NMR and concluded that there must be partial dissociation of the hydroxyl on the C6 for dissolution to occur [49]. Bialik et al. performed electrophoretic NMR measurements and molecular dynamics simulations on model cellulose substrates and found that the hydroxyl group on the C2 carbon is, to a large extent, deprotonated in aqueous alkali [50]. In relation to deprotonation, it is interesting to note that addition of other salts, such as Na_2SO_4, have been shown to suppress dissolution in NaOH(aq)[41]. This is a typical observation that can be made for polyelectrolytes when their charges are shielded, however surprising in this system due to the already high salt concentration, and has instead been discussed in terms of a salting-out effect as seen in proteins or cellulose derivatives [51].

Another feature of dissolution of cellulose in NaOH(aq) for which there is no clear explanation is the intriguing temperature dependency, i.e. that dissolution is promoted by decreasing temperature. One suggestion is that at low temperatures, there is a change in conformation around the C-C bonds of the glucose rings towards a more polar structure, which would minimize the hydrophobic assembly effect described under section 1.4 [24]. In a paper by Bergenstråhle-Wohlert et al., the conformation of cellotetraose in pure water (not including NaOH) was investigated by molecular dynamics simulations and NMR spectroscopy. It was found that both the orientation of the hydroxymethyl group, and the dipole moment of the glucose unit as a whole were relatively insensitive to temperature [52]. Another study of a model compound for cellulose, methyl β-D-glucopyranoside, dissolved in NaOH(aq), reported no significant conformation change of the hydroxymethyl group at low temperatures, based on the ^{1}H chemical shifts and ^{3}JHH couplings [53]. Thus, the contribution from a conformation change to the solubility remains uncertain. It is possible to instead seek the origin of the temperature dependency by examining the base and water structure. Yamashiki et al. measured the number of water molecules solvated to NaOH in the range of ca. 5 to 14 wt.% NaOH(aq), at + 4 °C and + 20 °C by NMR. It was found that the number of water molecules decreased with increasing NaOH concentration, and that more water molecules were solvating the NaOH at 4 °C compared to 20 °C [54].

With regards to the state of cellulose in solution, it is in general uncommon to have perfectly molecularly dissolved cellulose even in better solvents, however it seems that even low molecular weight cellulose is not well-dissolved in NaOH(aq). Even at low concentrations undissolved fractions can be separated [26]. Based on the rheology of microcrystalline cellulose (MCC) in NaOH(aq), this solvent was suggested by Roy et al. to yield suspensions and not true solutions [55]. Hagman et al. have used static light scattering (SLS), small angle X-ray scattering (SAXS) and NMR to measure the state of MCC in solution. They obtained conflicting results, as SLS showed aggregates in clusters of ca. 100 nm in rather dilute solutions, while the other measurements indicated molecularly dissolved chains [56].

Another issue with solutions of cellulose in NaOH(aq) is that they are not stable over time or when exposed to an increase in temperature. It has been shown that they gel or become turbid suspensions due to irreversible aggregation of the cellulose with increasing time and temperature [55]. In a study where gelation had been induced thermally, the gel-like solution was analysed using wide angle X-ray scattering (WAXS), and revealed that the aggregates were crystalline. It was suggested that the gel-like properties originated from crystal domains where cellulose chains participate in more than one domain, creating a network of physically linked chains. It was also shown that aggregation induced by an increase in temperature was not reversible by lowering the temperature [57]. Based on the these findings, the authors presented a hypothesis that the instability of the cellulosic solutions is because cellulose II has a lower solubility than cellulose I, leading to formation of cellulose II crystalline domains in the solution. The hypothesis is contradicted by an earlier study investigating the effect of crystal structure on solubility, showing that cellulose before and after mercerization was equally soluble. This study also reported that dissolution and regeneration of cotton linters in Cuen, which also results in formation of cellulose II, even improved solubility [58]. Here one also needs to consider that besides the crystal structure, the ultrastructure of the fibre changes upon dissolution and coagulation. In the same study it was, however, also indicated that precipitates formed by heat could not be redissolved upon cooling. Therefore, it is not entirely simple to conclude the impact of crystal structure on solubility.

Regarding the dissolution rate, in NaOH(aq) diffusion of the solvent into the cellulose will be fast compared to, for example, ionic liquids. In the work by Wang et al. the diffusion coefficient of Na^+ in NaOH/urea(aq) was reported to be 3.8×10^{-10} m^2/s at 0 °C without cellulose [59]. According to a study by Lovell et al., the diffusion coefficient of the cation in the ionic liquid EmimAc was reported as 9.6×10^{-12} m^2/s without cellulose [60]. Here, it can be noted that the fast diffusion of the aqueous hydroxide solvents likely contribute to comparably fast dissolution. The exact kinetics of dissolution is rarely stated, however in the work by Wang et al. the solubility of cotton linters in NaOH(aq) solutions was measured as a function of time and temperature, and dissolution occurred within 30 min [61].

Besides NaOH, LiOH can also dissolve cellulose under conditions similar to NaOH (temperatures below 0 °C, ca. 2 M(aq) base concentration) and has been reported to show slightly better solution properties and dissolution capacity compared to NaOH(aq) [38]. It has not received as much attention as the NaOH(aq) system, probably because the use of NaOH is more attractive to industry. Unlike NaOH and LiOH, KOH cannot dissolve cellulose and again, the reason is not fully understood. In a paper by Xiong et al., it was observed that there is a difference in the hydration shells of the bases, and it was hypothesised that as a consequence, cellulose can form a stable complex with NaOH and LiOH, but not with KOH [47].

Quaternary ammonium hydroxides(aq)

Similar to NaOH, aqueous solutions of quaternary ammonium hydroxides (QAHs) were also found to be able to dissolve cellulose in the early 20th century, as can be seen in another patent by Leon Lilienfeld [62]. Interestingly, he found that aqueous solutions of 20-50 wt.% of tetraethyl-, tetramethyl- and phenyltrimethylammonium hydroxide could dissolve cellulose either at temperatures below 0 °C or at room temperature, depending on the cellulose employed. This shows that already at this time in history, the intriguing inverse temperature dependency was also found for the QAHs, but that in some cases higher temperatures could be used. Soon after this, Powers et al. patented the use of benzyl substituted ammonium hydroxide solutions because it was found that these bases were even better solvents for cellulose than NaOH(aq), or for example tetramethylammonium hydroxide (TMAH)(aq). Already it was being concluded that even though these benzyl substituted quaternary ammonium hydroxides must be soluble in water in order to give strong basic solutions, the solvent action of the bases was not solely dependent on their basicity. Two of the bases mentioned in this patent were trimethylbenzylammonium hydroxide and dimethylbenzylphenylammonium, named Triton B and Triton F (see Figure 1.6)[63].

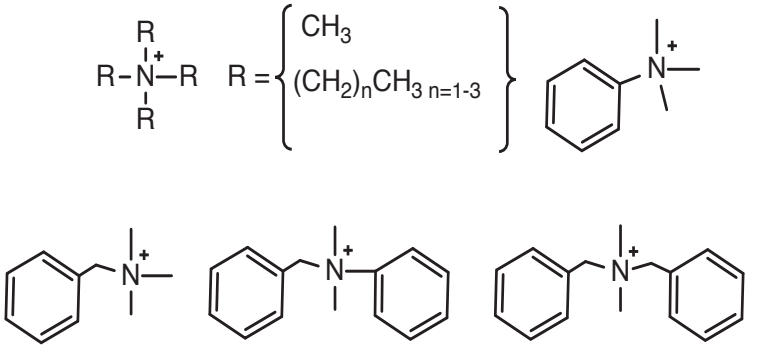

Figure 1.6: Starting from the upper left, structure of the cations in: tetramethyl/ethyl/propyl/butyl ammonium hydroxide, trimethylphenyl-, trimethylbenzyl-, dimethylbenzylphenyl- and dimethyldibenzyl ammonium hydroxide.

The solvent action of Triton B and Triton F was further investigated by Brownsett and Clibbens who found two solubility maxima, a feature sometimes seen for the QAHs as opposed to the alkali hydroxides with only one maxima. Similar to NaOH, the dissolution capacity increased with decreasing temperature. The concentrations of base where maximum dissolution occurred, decreased with decreasing dissolution temperature. Another finding was that with increasing molecular weight of the base, the solvent power and the viscosity of the aqueous solutions of the bases, at a given molar concentration increased. This was explained by the introduction of a large molecule between the cellulose chains [64]. This was then investigated by Sisson and Saner through the use of X-ray diffraction. It was found that immersing the cellulose in the solvents was accompanied by an extension of the crystalline lattice. However, no significant difference was found in the extension when bases with small or large molecular volumes were compared [65]. A more recent study by Wang et al. investigated dissolution in aqueous solutions of tetramethyl-, triethylmethyl-, tetraethyl-, benzyltriethylammonium hydroxide as well as Triton B and the alkali bases in up to 1.8 M base. It is stated that for all of these bases, dissolution required low (freezing) temperatures. However it was not stated if more concentrated base solutions were tested. Through this series of QAHs, the same results were reached as with Brownsett and Clibbens, however it showed that as the base increases in molecular weight it is accompanied by an increase in hydrophobicity. The hydrophobicity is in turn the reason behind the increasing solubility and stability [66]. Because of the amphiphilicity of cellulose, this increase in hydrophobicity helps to stabilize the more hydrophobic regions of the pyranose ring and prevent the aggregation of cellulose caused by hydrophobic stacking.

In a similar study, Zhong et al. compared the solubility of cellulose in more concentrated solutions of four non-benzyl substituted QAHs with increasingly hydrophobic chains from methyl groups to butyl groups. In this case dissolution required room temperature or higher. The most hydrophobic base, tetrabutylammonium hydroxide, was the best solvent, however the discussion of the mechanisms of dissolution centered around hydrogen bonding capability. The authors measured the Kamlet-Taft parameters of the solvents (indicative of hydrogen bonding and van der Waals interactions). They report that an increasing β-value (indicative of the hydrogen bond acceptor ability) gave an increasing cellulose solubility [67]. It can be noted that the bases were compared on a weight

percent basis, but since the bases have different molecular weights, the molecular interactions must reasonably be determined by the number of moles rather than the weight of the base.

A study regarding the state of cellulose when dissolved in QAHs looked at pulp in TBAH(aq) and reported molecularly dissolved cellulose at lower cellulose concentrations through the use of static light scattering measurements [68]. In another study the hydrodynamic size of cellulose in QAHs was measured via dynamic light scattering and at 0.2 g/L, it was reported that the cellulose was molecularly dissolved [66].

Quaternary phosphonium hydroxides (QPHs) have also been reported to dissolve cellulose. However, they have not been as extensively investigated as the QAHs, one possible reason could be that the QAHs are more readily commercially available. The QPHs do however seem promising and comparable to the QAHs, as for example a tetrabutylphosphonium hydroxide (TBPH) solution of 60 wt.% (aq) was reported to have a dissolution capacity similar to concentrated TBAH(aq) at 25 °C [69]. In another study it was shown that 50 wt.% TBPH(aq) can dissolve cellulose within the temperature range of 0 to 50 °C. It was also shown that, similarly to the QAHs, there are several different QPHs that can dissolve cellulose, one example being tetraethylphosphonium hydroxide [70]. In another study of TBPH the stability of the base was investigated and it was shown that it decreases with increasing base concentration and temperature. At 40 to 50 wt.% TBPH, it was stable for up to 90 °C, but for more concentrated solutions decomposition of the base occurred [71].

Additives

Because of the poor dissolution capacity of NaOH(aq) and the stability issues of the cellulosic solutions, different additives such as ZnO [72] [73], urea [38], thiourea [74] and PEG [75] have been used to improve dissolution. The ones that have received the most attention are ZnO and urea, and their action on cellulose dissolution will be described in this section.

Zinc oxide

As early as 1937 Davidson reported that concentrated and stable solutions of modified cotton could be prepared in NaOH(aq) solutions containing zinc oxide (ZnO). Besides ZnO, beryllium oxide and aluminium oxide were also added to NaOH(aq) solutions. Beryllium oxide was found to increase dissolution but not to the level of zinc oxide. Aluminium oxide on the contrary impeded dissolution [72]. More recent investigations into NaOH/ZnO(aq) solutions have reported that the addition of ZnO delays the gelation of the solutions and suggested that ZnO acts as a water binder [76]. In another study it was found that ZnO exists as $[Zn(OH)_4^{2-}][Na^+]_2$ in these strongly alkaline solutions and that the $Zn(OH)_4^{2-}$ formed hydrogen bonds with cellulose. It was also suggested that the hydrogen bonds between $Zn(OH)_4^{2-}$ and cellulose are stronger than those between NaOH and cellulose [73].

Urea and urea derivatives

If urea is added to NaOH(aq), cellulose with a higher molecular weight can be dissolved compared to when only NaOH(aq) is used [38]. The addition of urea has also been shown to delay (but not prevent) gelation, increasing the stability of the solutions [77]. Thiourea has also been used as an additive to NaOH(aq) solutions and gelation of cellulose dissolved in NaOH/urea/thiourea was

investigated by Zhang et al. [78]. The choice of additive has also been shown to have an effect on the temperature at which dissolution occurs. Jiang et al. found that with thiourea dissolution occurred at 8 °C instead of at - 5 °C with urea. In the same study, DLS measurements of dilute solutions of cellulose in NaOH/thiourea(aq) revealed the presence of aggregates, and showed that as for in NaOH(aq) without additives, not all of the cellulose was molecularly dissolved [74]. Urea and ZnO have also been used together as additives to NaOH solutions and were found to increase the dissolution capacity of cellulose in the solvent [73].

As for the NaOH(aq) and LiOH(aq) solutions, urea and derivatives of urea have been used as an additive to improve dissolution in both QAH- and QPH(aq) solutions. Sirviö and Heiskanen have reported that not only urea, but also N-methylurea, N-ethylurea, 1,3-dimethylurea and imidazolidone were found to improve dissolution of cellulose when dissolved in tetraethylammonium hydroxide(aq) solution [79].

As previously mentioned, the use of aqueous hydroxide base solvents have not reached industrial scale but there are initiatives to do so. Two of them are the BioCelSol process and TreetoTextile. BioCelSol utilizes a mechanical and enzymatic pretreatment of pulp to dissolve it in NaOH/ZnO(aq) [80]. TreetoTextile appears to utilize NaOH(aq) with or without additives, based on their patented technology [81].

Combinations of hydroxide bases

There are few reports on combining hydroxide bases in aqueous solution to dissolve cellulose. One is a note in the patent of Lilienfeld, mentioning that addition of alkali hydroxides to QAH solutions can enhance dissolution of cellulose, but without giving further details [62]. The other is in the article by Davidson in 1936, where he investigated a combination of NaOH with LiOH and for concentrations of 3.5 and 4.0 N, a maximum in solubility could be observed for a molar ratio of 0.5 [41].

2 Materials and methods to investigate the dissolution of cellulose and the properties of the solutions

The material and methods used throughout this thesis will be briefly explained in this chapter, but the reader is referred to the appended articles for more detailed descriptions.

2.1 Materials

A microcrystalline cellulose (MCC) of the type Avicel PH-101 was purchased from SigmaAldrich and used throughout this thesis, with an exception for some of the NMR measurements that were performed on a model cellulose substrate. As stated by the manufacturer, the Avicel PH-101 is a purified and depolymerized cellulose made by the partial acid hydrolysis of wood pulp [82]. It was sent for molecular weight analysis through size exclusion chromatography in DMAc/LiCl to two different labs (performed by Södra Cell and MoRe Research), and the results were as seen in Table 2.1.

Table 2.1: Number-, weight- and zeta- average molecular weight [g/mol] of the MCC and the corresponding degree of polymerisation.

Avicel pH-101			
M_n	$11.7 - 14.8 \times 10^3$	DP_n	72-90
M_w	$29.0 - 56.0 \times 10^3$	DP_w	180-350
M_z	$58.0 - 145 \times 10^3$	DP_z	360-895

The MCC was chosen because it is soluble in most solvents for cellulose and widely employed when studying dissolution of cellulose, which facilitates comparison between the investigated solvents. The other chemicals used were purchased from large suppliers and used as received, the details of which can be found in the appended papers.

2.2 Methods

2.2.1 Dissolution of cellulose

In order to dissolve cellulose in the solvent systems investigated, the temperature must be brought below room temperature. This was achieved by various methods depending on the purpose of the investigations. When the temperature dependency was investigated, the temperature of the solvent was set by immersing it in a temperature controlled oil bath (Julabo F25). When the exact temperature dependency of the dissolution process was not under investigation, the solution was cooled in an ice bath and then stored in a freezer at -20 °C for enough time to bring the temperature of the sample down to circa - 10 °C (20 minutes for a sample size of 10 ml).

2.2.2 Maximum dissolution capacity

Two different methods were used to estimate the maximum amount of cellulose that could be dissolved. The first method was the inspection of solutions with increasing amounts of cellulose using a light microscope, in order to observe the occurrence of undissolved particles. The dissolution limit was set to when tenfold of undissolved fibres were observed (see Paper I [83]). The second method was to prepare solutions of increasing amounts of cellulose and centrifuge them in order to separate the undissolved particles from solution and weigh them. The dissolution limit was then set to when more than 15 wt.% of the cellulose was undissolved (due to that in NaOH(aq), there was always a small fraction of undissolved fibres) (see Paper II [84]).

2.2.3 Methods to measure the size and conformation of cellulose in the dissolved state

Dynamic light scattering
The effective hydrodynamic radius (R_h) was measured through dynamic light scattering (DLS) using a Zetasizer Nano ZS from Malvern Panalytical with a 4 mW, 632.8 nm red laser at a scattering angle of 175°at 20 °C. The solvents were filtered with 0.22 μm filters before addition of cellulose to minimise dust in the samples. After preparation of the cellulose solutions, they were measured directly and both unfiltered or filtered using a 1.2 μm acryclic copolymer filter or a 0.22 μm polyether sulfone filter. The concentration measured was kept at a fixed molar ratio of 268 mol base per anhydroglucose unit (AGU) and 24 mol H_2O per mol base, corresponding to ca. 1.4×10^{-3} g/ml in a 2 M solvent. The viscosity of each solvent was measured at 20 °C through flow sweeps and the measured viscosity was used for the data analysis. The refractive index of the solvents was measured with an Abbemat 550 from Anton Paar using a wavelength of 589 nm at 20 °C and was also used as an input for the data analysis.

Static light scattering
The zeta average radius of gyration ($R_{g,z}$) and the weight average molecular weight (M_w) were obtained through static light scattering (SLS) measurements using a CGS-8F from ALV GmbH with a 50 mW laser operating at a wavelength of 532 nm. The measurements were made at a scattering angle of 17° to 152° with a maximum step size of 4°, and the temperature of the sample cell was 7 °C. The cellulose solutions were measured directly after preparation at concentrations in the range of 5×10^{-4} to 1.6×10^{-2} g/ml and measured either unfiltered or filtered using a 1.2 μm acrylic

copolymer filter or a 0.22 μm wwPTFE filter. Each concentration was prepared individually and not diluted from a stock solution. The refractive index was measured as detailed for DLS.

Small angle X-ray scattering
The conformation of the cellulose was measured using Small angle X-ray scattering (SAXS) and were performed on a Mat:Nordic from SAXSLAB with a Rigaku 003+ high brilliance microfocus Cu-radiation source and a Pilatus 300K detector. Samples of dissolved cellulose were always prepared in direct conjunction to the SAXS measurement and measured within 8 hours while under temperature control (using a JULABO recirculating bath with a cooling liquid). The measured q-range was 0.007 – 0.25 $Å^{-1}$, the two-dimensional scattering pattern was radially averaged using either the SAXSGui software or in PyFAI and the sample data was subtracted by the solvent data. The concentrations of cellulose ranged between 1 to 2.5×10^{-2} g/ml. The modelling of the data was performed using SasView.

2.2.4 Methods to measure the stability of the solutions

Different types of measurements were performed in order to investigate the rheology of the solutions, as it is indicative of polymer solvent interactions and important for applications.

Oscillatory dynamic rheology measurements, where the evolution of the storage modulus (G') and loss modulus (G") of the solutions was measured over time, were used to measure the stability of the solutions over time. This allows detection of gelation when the storage and moss modulus cross (G' = G"). A TA Discovery Hybrid Rheometer (HR-3), with a sandblasted 40 mm plate-plate geometry with a gap of 1 mm was employed and the temperature was controlled by a Peltier plate with circulating cooling liquid. The concentrations measured were 3 and 5 wt.% MCC. After performing strain sweeps an angular frequency of 1 rad/s and a strain of 10% were chosen for samples with 3 wt% MCC, and an angular frequency of 1 rad/s and a strain of 1% for samples with 5 wt% MCC. At 3 wt.% MCC the signal was low and close to the detection limit. Samples were measured directly after dissolution with a water-filled solvent trap and brought to the desired temperature in the rheometer without pre-shearing.

Rotational rheology measurements, where the viscosity was measured as a function of shear rate, were used to investigate the flow behaviour of the solutions in order to determine if they behaved as Newtonian solutions or exhibited shear thinning. The same instrument and instrument set-up used for oscillatory measurements was used, and the samples were measured directly after dissolution. The measurements were conducted with shear rates from 1 to 100 $[s^{-1}]$, at increasing temperatures.

Intrinsic viscosity was measured to investigate if the observed solution properties were reflected in the expansion of the cellulose chains in the solvent. A capillary viscometer with circulating water was used at 25 °C. Cellulose concentrations in the range of 0.1 to 1.1 g/dL were measured and the solutions were placed in a 25 °C water bath directly after dissolution for 30 min before the measurements. Three measurements were made for each sample and the average was used to calculate the relative viscosity, which was determined with a maximum error of 2%. The intrinsic viscosity was obtained from linear regression with a coefficient of determination of at least 0.97.

The stability of solutions over time and against an increase in temperature was also monitored by following the transmission of light through the solutions. A SPECORD 205 UV-VIS spectrophotometer from Analytik Jena was used and the measurements conducted at room temperature. Plastic disposable cuvettes with a light path length of 10 mm were used throughout the measurements, and water was used as the background. A scan was performed over a range of 250 to 1100 nm. The transmission at 800 nm was selected as the measurement point since neither the dissolved cellulose or the solvent absorbed light there. For studies of the temperature stability, the solution was kept in the dissolution vessel and the temperature of the solution was raised during stirring in 10 °C steps, to a maximum of 75 °C. The transmission was measured at each step as soon as the solution had reached the desired temperature. The entire procedure, starting from when the cellulose had been dissolved at – 5 °C for 30 minutes, took ca. 2.5 h. For measuring the stability over time the cellulose was transferred to a beaker after the dissolution step at – 5 °C and stored at the desired temperature (8 °C in a fridge, 20 °C at room temperature or 35 °C in an oven) without stirring.

2.2.5 Characterisation of the solvent structure and interactions with cellulose

Differential Scanning Calorimetry (DSC) was employed to identify the melting temperature of hydrates in solution and correlate them to their structure. This was measured for solutions with and without cellulose. The enthalpy was obtained from the peak area in the obtained thermoscans and correlates to the amount of the hydrate in solution. Thermoscans were performed using a DSC 250 from TA Instruments Discovery series equipped with stainless steel pans. The samples were cooled using a cooling rate of 10 °C/min down to - 70 °C, and kept at - 70 °C for 5 min, before heating again at 1 °C/min.

1D ^{1}H and ^{13}C solution Nuclear Magnetic Resonance (NMR) spectroscopy was employed in order to investigate how the bases interacted with a glucose model of cellulose in solution. The samples were methyl-α-D-glucopyranoside (0.4 M) dissolved with ca. 2 M NaOH, 2 M TMAH or 2 M 50/50 mol% NaOH/TMAH in D_2O. The measurements were run on an 800 MHz magnet equipped with a Bruker Avance HDIII console and a TXO cryoprobe. Spectra were recorded with a low angle radio frequency pulse to minimize relaxation weighting using a single pulse experiment with ^{1}H decoupling during acquisition and a relaxation delay set to 5 s; 8 scans were collected. A capillary containing D_2O with 3-(trimethylsilyl)-1-propanesulfonic acid sodium salt (DSS) was placed inside the tube as an internal reference.

Solvatochromic dyes, which change their absorption in the UV-visible range depending on the interactions with the solvent, were used to estimate the possible hydrogen bonds and van der Waals interactions between cellulose and the solvents. The dyes 4-nitroanisole (1), N,N-diethyl-4-nitroaniline (2), 4-nitroaniline (3) and Reichardt's dye (4) (see Figure 2.1) were used to obtain the parameters α, β, and π (see Equations 2.1 - 2.4). The dye pairs (2) and (3) were used to obtain β and the pair (1) and (4) to obtain α. Concentrated solutions (20 mg/5 ml) of the dyes 4-nitroanisole and 4-nitroaniline were prepared in water, while for Reichardt's dye ethanol was used instead of water due to poor solubility. A small aliquot of these concentrated solutions (0.2 μL) was added to cuvettes containing 1.5 ml of the sample and stirred before being measured. N,N-diethyl-4-nitroaniline was added directly to the samples to be measured. The instrument used for measurements at room

temperature was a SPECORD 205 UV-VIS spectrophotometer from Analytik Jena. Measurements with temperature control were conducted on a Cary 4000 spectrophotometer from Agilent. Plastic disposable cuvettes with a light path length of 12.5 mm were used throughout the measurements, and water was used as the background. The maximum absorption of the peaks of interest ranged from 0.1 to 1.1.

$$\pi_1^* = \frac{34.12}{2.343} - \frac{10,000}{2.343 * \lambda_{max,1}} \tag{2.1}$$

$$\pi_2^* = \frac{27.52}{3.182} - \frac{10,000}{3.182 * \lambda_{max,2}} \tag{2.2}$$

$$\beta = \frac{1.035v(\pi_2^*) + 2.64 - v(\beta)}{2.80} \tag{2.3}$$

$$\alpha = \frac{v(RD) + 1.873v(_1^*) + 74.58}{6.24} \tag{2.4}$$

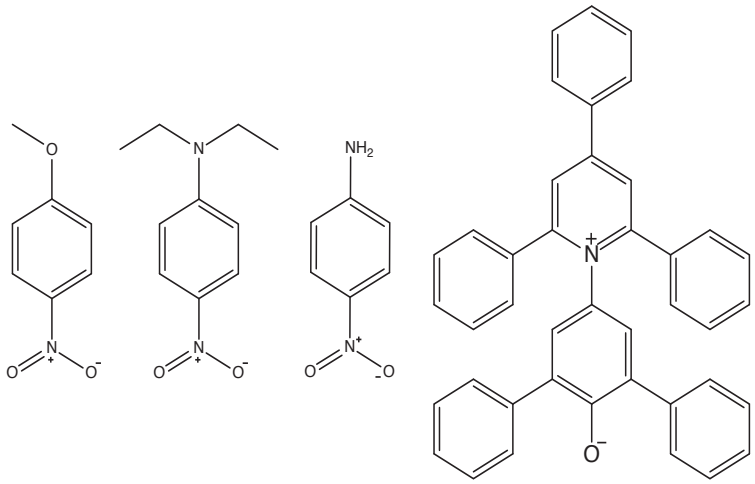

Figure 2.1: From left to right: 4-nitroanisole (1), N,N-diethyl-4-nitroaniline (2), 4-nitroaniline (3) and Reichardt's dye (4).

2.2.6 Methods to measure the crystalline structure of cellulose, both swollen and fully coagulated

X-ray diffraction was used to measure the crystalline structure of cellulose before and after dissolution as well as in a swollen state. Measurements of the swollen cellulose samples were performed using a Mat:Nordic from SAXSLAB with a Rigaku 003+ high brilliance microfocus Cu-radiation source and a Pilatus 300K detector. The cellulose concentration was 1 g/6 ml of 4 mol% solvent, either measured in capillaries or in a sandwich cell where the cellulose sample was clamped between two Kapton windows.

The samples were stored at room temperature for at least 2 h, + 3 °C for 22 h or -20 °C for 3 h before being measured. The measured q-range was 4×10^{-3} - 2.3 $Å^{-1}$, the two-dimensional scattering pattern was radially averaged using the SAXSGui software and the sample data was subtracted by the solvent and sample holder data, unless otherwise stated.

Solid-state NMR measurements were performed on the same type of sample swollen at -20 °C as for X-ray diffraction. The measurements were conducted on a Bruker Avance III 500, operating at 500.13 MHz ^{1}H and 125.76 MHz ^{13}C, equipped with a 4 mm HX CP-MAS probe. Measurements were conducted at 298 K with a MAS spinning rate of 10 kHz. A cross-polarization magic angle spinning (^{13}C CP/MAS) pulse sequence with a SPINAL-64 decoupling sequence was used with acquisition parameters including a 3.0 ^{1}H pulse, a 1500 CP-contact time, 7-23 ms acquisition time, 20000 scans, and 3 s recycle delay. The chemical shifts were referenced to adamantane with CH_2-signal set to 38.48 ppm.

For fully coagulated samples, cellulose was first dissolved at a concentration of 10 g/L in 2 M aqueous base solution at -5 °C, coagulated using HCl(aq), filtrated and washed with deionized water until the filtrate was pH neutral. The cellulose was then dried at 45 °C overnight. X-ray diffraction was measured using a D8 Advance from Bruker, equipped with a 1.54 Å Cu source with a First gen Lynx-eye PSD detector. The samples were ground using a hand mortar, placed on a low background silica holder, and subjected to radiation at 40.0 kV and 40.0 mA. The scan range was 5 – 45 °with a step size of 0.05°á 2 s (except for 0.1°á 8 s for the cellulose regenerated from NaOH). The software used for the analysis was DIFFRAC.EVA v5.2.

3 Results and Discussion

3.1 Combining bases

As discussed in the introduction, one of the objectives of the work was to further understand the role of the cation for dissolution of cellulose in aqueous hydroxide bases. As presented in the theory and background, the quaternary ammonium hydroxides provide better dissolution than NaOH, and therefore another objective was to explore the idea that a quaternary ammonium hydroxide can be combined with NaOH to give the same positive effect as an additive. However, previous studies dealing with this approach were scarce, so at first it had to be determined if it would be possible to combine bases without disturbing dissolution. As also detailed in the theory and background, dissolution of cellulose in NaOH(aq) only occurs within a narrow concentration interval with an optimum at ca. 2 M NaOH(aq). Therefore in the initial trials only a small portion (10 mol%) of the NaOH was replaced with another base so as to keep the total NaOH concentration within the known dissolution interval. It was then discovered that even 50 mol% of the NaOH could be replaced while still retaining the dissolution ability, despite the fact that a 1 M NaOH(aq) will not dissolve cellulose. After this discovery, an initial investigation was performed where 50 % of the NaOH in a 4 mol% (2 M) solution was replaced with a few selected, commercially available quaternary ammonium/phosphonium hydroxide bases and tested for dissolution of cellulose through simple visual inspection of the solutions (see Table [3.1]). The studied bases were tetramethylammonium hydroxide (TMAH), benzyltrimethylammonium hydroxide (Triton B), tetrabutylphosphonium hydroxide (TBPH) and tetrabutylammonium hydroxide (TBAH) (see Figure 3.1 for their structures). It should be noted that when reporting the concentrations in this thesis, at times Molar (mol/L) is used and other times mol% (or mol ratio). This is due to the fact that when bases have a significant difference in molar volumes, a comparison at the same mol% was deemed more accurate.

Table 3.1: The combination of bases or individual bases that could dissolve cellulose at low temperatures at a total base concentration of 4 mol%.

Base	NaOH	TMAH	Triton B	TBPH	TBAH
NaOH	Yes	Yes	Yes	No	No
TMAH	-	Yes	Yes	Yes	No
Triton B	-	-	Yes	Yes	No
TBPH	-	-	-	Yes	No
TBAH	-	-	-	-	No

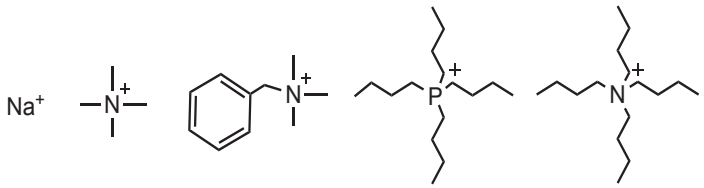

Figure 3.1: Structure of the cations in NaOH, TMAH, Triton B, TBPH and TBAH.

Two of the studied combinations were successful, NaOH with TMAH and NaOH with Triton B. The dissolution of cellulose in 2 mol%(aq) solutions of pure NaOH and pure TMAH was also tested (see Figure 3.2). It was confirmed that at these concentrations they cannot dissolve MCC, and therefore must be cooperating in the combined solution. Noteworthy is the fact that while tetrabutylammonium hydroxide (TBAH) could not dissolve the MCC on its own under the low temperature applied (or at room temperature), TBPH could do so. A test was also made where NaOH was combined with KOH to investigate if it would be possible to use a cation that cannot usually dissolve cellulose, however it was unsuccessful. As can be viewed in Table [3.1], it was also possible to combine two quaternary ammonium hydroxides to dissolve cellulose, but because NaOH is nontoxic, low-cost, and readily available, the continued investigation focused on the combinations with NaOH.

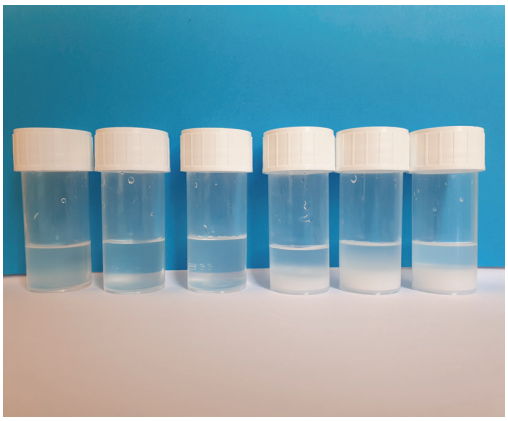

Figure 3.2: From left to right: 3 wt% MCC in ca. 4 mol% NaOH(aq), 50/50 NaOH/TMAH(aq), TMAH(aq) and 2 mol% NaOH(aq), 50/50 mol% NaOH/TMAH(aq) and TMAH(aq).

3.2 How much cellulose can be dissolved?

In order to investigate the effect of combining bases on the amount of MCC that could be dissolved, the maximum dissolution capacity for individual bases and base combinations was determined. As a comparison, the dissolution capacity for the single-base solvents with the additive urea was also measured. Finally, the effect of adding urea to the combinations was also measured to shed light on the mechanisms in the solutions. Regarding the method, there are several different ways of measuring the maximum dissolution capacity and common methods reported in literature are qualitative visual inspection by eye or microscope [66][67][79], turbidity measurements [85], or quantification of undissolved fibres through centrifugation of the solutions [78][74]. All these methods will give different dissolution limits as they are sensitive to different solution properties (e.g. particle size, viscosity etc.), but applying the same method for a series of samples should allow for internal comparison. Here, the results from using a centrifugation method are presented in Table [3.2] (see Paper II for details).

Table 3.2: The maximum dissolution capacity of MCC in the specified solvent as determined through the centrifugation method, in weight %, Molar and mol base per mol AGU at maximum dissolution. The solvents with urea had a composition of ca. 4 mol% base and 4.5 mol% urea(aq).

Solvent(aq)	Max wt.% MCC	Max mol MCC per L solvent	mol base/mol AGU
4 mol% NaOH	2.0 (3[1])	0.12	16.6
4 mol% TMAH	2.7 (6[1])	0.17	11.0
4 mol% NaOH/Triton B (50/50)	3.1	0.20	9.3
4 mol% NaOH + urea	3.5	0.24	8.3
4 mol% NaOH/TMAH (50/50)	4.2 (5[1])	0.27	7.4
4 mol% NaOH/Triton B (50/50) + urea	4.2	0.28	6.1
4 mol% TMAH + urea	4.9	0.32	5.3
4 mol% NaOH/TMAH (50/50) + urea	6.1	0.41	4.4
4 mol% Triton B	6.8	0.44	3.7
4 mol% Triton B + urea	6.8	0.46	3.3

The dissolution capacity of the individual bases was found to increase with an increase in hydrophobicity of the cation (NaOH<TMAH<Triton B), in line with the results reported by Wang et al. [66]. Combining NaOH with TMAH had a synergistic effect on dissolution and increased the dissolution capacity beyond that of NaOH(aq) or TMAH(aq). Combining NaOH with Triton B increased the dissolution capacity beyond that of NaOH(aq), but the capacity was significantly below that of Triton B(aq). It should also be noted that the dissolution capacity of NaOH combined with TMAH was greater than for NaOH combined with Triton B. Considering the fact that as a single-base solvent, Triton B was superior to TMAH, this was an unexpected result and indicated that the interactions between the bases need to be considered.

[1] As measured by qualitative inspection by microscopy.

The effect of adding urea to the solutions was a significant increase in the dissolution capacity of solvents containing NaOH or TMAH, but no significant effect could be observed for solutions of pure Triton B(aq), as opposed to what has been reported for other QAHs [79]. The increased dissolution capacity of the 50/50 NaOH/Triton B(aq) solvent upon the addition of urea could likely be attributed to the effect of urea on NaOH.

The dissolution limit for 4 mol% NaOH(aq), TMAH(aq) and 50/50 NaOH+TMAH(aq) was also estimated by assessing the occurrence of undissolved particles with a microscope, a more qualitative method (see Table 3.2 and Paper I [83]). For the NaOH(aq) and 50/50 NaOH/TMAH(aq) solutions, the results were reasonably consistent with those obtained through centrifugation (see Table 3.2). However, the dissolution limit for the TMAH(aq) solution was higher when determined with microscopy. This might be due to swollen aggregates in the TMAH(aq) solutions that were not visible through a microscope, but large enough to be separated through centrifugation, and highlights the fact that depending on the method chosen, the dissolution limit can differ.

As mentioned in the theory and background, different solvents have different molar volumes. Therefore, the dissolution capacity in terms of mol MCC per litre of solvent is also given in Table 3.2 for comparison. The number of moles of base per AGU at the dissolution limit is also stated to show that, for example, in the case of NaOH or TMAH, it is not a shortfall of base that limits dissolution.

3.3 Properties of the solvents as measured through solvatochromic dyes

In order to explain the observations on dissolution capacity, solvatochromic dyes were used to measure the solvatochromic parameters π^*, β and α, the so-called Kamlet-Taft parameters. These parameters are based on the interaction between the dyes and the solvent and could give indication on possible interactions in terms of polarity/polarizability and hydrogen bonding between cellulose and the solvents. It can be noted that there are numerous dyes that can be used to determine these interactions, but one should not compare the absolute values obtained from different dyes but should rather compare trends, as demonstrated by Rani et al. [86].

Polarity and polarizability

The π^* parameter measures the polarity and polarizability of the solvent, increasing with increasing polarizability and polarity [87]. Two different dyes were used to obtain π^* since they were both needed for subsequent determination of α and β. The obtained values are listed in Table 3.3. It is difficult to see a trend in π^* that agrees with the dissolution capacities since an increase in the hydrophobicity of the bases should mean a decrease in polarity, however π^* is also affected by polarizability. This can be seen when comparing the solutions of TMAH and Triton B: Triton B is more hydrophobic and less polar, but despite this a higher π^*-value was observed for Triton B than for TMAH, which can be attributed to Triton B being more polarizable due to the benzyl group with delocalised electrons. It is difficult to judge what effect this polarizability could have on dissolution.

For both probes, addition of urea generally increased π^*, which could be explained by urea being more polarizable than water, with the exception of the Triton B solution, which appeared to be unaffected. This could be indicative of a relatively strong interaction between Triton B and the π^* probe, excluding urea from also interacting with the probe. This could possibly explain the observation that adding urea to Triton B did not seem to have a significant effect on cellulose dissolution, as urea might be excluded from interacting with cellulose in the presence of Triton B.

Table 3.3: The π^* parameters for the specified solvent and the difference in π^* for the same solvent with urea (4 mol% base, 4.5 mol% urea(aq)), obtained at room temperature. π_1^* was obtained using the dye 4-nitroanisole and π_2^* using N,N-diethyl-4-nitroaniline.

4 mol% solvent at RT	π_1^*	π_2^*	$\Delta\pi_1^*$	$\Delta\pi_2^*$
H_2O	1.06	1.31	0.10	0.07
NaOH	1.12	1.36	0.11	0.05
TMAH	1.08	1.30	0.07	0.03
Triton B	1.22	1.39	0.02	0.01
50/50 NaOH/TMAH	1.08	1.35	0.11	0.02
50/50 NaOH/Triton B	1.14	1.40	0.04	0.01

Hydrogen bonding - acceptor ability

The β parameter measures the hydrogen bond acceptor ability of the solvent [88]. Both water and urea are hydrogen bond acceptors and hydrogen bond donors. The hydroxide ion is however a stronger hydrogen bond acceptor than water or urea and its interactions should thus dominate the β parameter. Despite the fact that all the bases have the same hydroxide anion and concentration, their β-values differed and the single-base solvents followed the same trend as the dissolution capacity, with the highest β values obtained for solutions of Triton B (Table 3.4). One possible explanation is that a more hydrophobic cation decreases the hydration of the hydroxide ion, effectively increasing its activity. This should be favourable in interacting with the hydroxyl groups on cellulose. Regarding the combined solvents, a β value corresponding to an average of the two single-base solvents was obtained. This indicates that the properties of the combined solvents (such as improved dissolution capacities) do not stem from an effect on the hydroxides ability to hydrogen bond. The addition of urea to water slightly increased β, indicating that compared to water, urea was a slightly better hydrogen bond acceptor. When both urea and base were present there was no effect on β, probably owing to the fact that urea cannot compete with the hydroxide ion as a hydrogen bond acceptor.

Table 3.4: The β parameter for the specified solvent and the difference in β for the same solvent with urea (4 mol% base, 4.5 mol% urea(aq)), obtained at room temperature.

4 mol%(aq) solvent at RT	β	$\Delta\beta$
H_2O	0.13	0.04
NaOH	0.20	0.01
TMAH	0.31	-0.02
Triton B	0.38	-0.01
50/50 NaOH/TMAH	0.24	0.00
50/50 NaOH/Triton B	0.31	-0.01

Hydrogen bonding - donor ability

The α parameter measures the hydrogen bond donor ability of the solvent [89]. As previously mentioned, water and urea can act as hydrogen bond donors as evidenced by their high α values (Table 3.5). The base solutions have significantly lower α-values compared to pure water, despite the fact that they contain 96 mol% water. The low α value of the NaOH(aq) solution might possibly be explained by competition between the dye and the hydroxide ion for hydrogen bond donation by water, with the hydroxide ion being favored. When comparing the bases, α increased in the order of $Na^+ < TMA^+ << TritonB^+$ at 4 mol% base. None of the cations investigated here have hydrogens capable of conventional hydrogen bonding, although the hydrogens on the organic cations could act as weak donors. Another factor could be the hydration of the bases, if the more hydrophobic bases are less hydrated, this could increase the possibility for Lewis acid activity of the cation, since the positive charge is not as shielded. The Lewis acid activity could also affect the absorption spectra of the dye. A third effect could come from the structure of the water (not the amount, which was the same). So-called dangling water, with fewer hydrogen bonds, is commonly observed in the hydration shell of hydrophobic solutes [90]. This water might possibly be more prone to hydrogen bond to the alkoxide of the dye, affecting α.

Table 3.5: The α parameter for the specified solvent and the difference in α for the same solvent with urea (4 mol% base, 4.5 mol% urea(aq)), the values are an average of values obtained at 15 and 35 °C.

4 mol%(aq) solvent	α	$\Delta\alpha$
H_2O	1.05	-0.10
NaOH	0.24	-0.11
TMAH	0.28	-0.08
Triton B	0.55	0.03
50/50 NaOH/TMAH	0.26	-0.05
50/50 NaOH/Triton B	0.69	-0.04

An additional, higher base concentration was therefore measured to see the effect on α (see Table 3.6). As the concentration of base was increased, α decreased for NaOH and TMAH but remained at the same level for Triton B. The decrease in α for NaOH and TMAH could come from a decrease of the concentration of water, or an increase in the concentration of hydroxide ions. The fact that α remained high for Triton B could possibly originate from interaction with the positive charge

but it is difficult to draw steadfast conclusions here. With regards to urea, the addition to water decreased α, indicating that compared to water, urea is a weaker hydrogen bond donor.

Table 3.6: The Kamlet-Taft parameters for increasing concentrations of base, obtained at room temperature (*average of values obtained at 15 and 35 °C).

Solvent(aq)	π_1^*	π_2^*	β	α
4 mol% NaOH	1.12	1.36	0.20	0.24*
8 mol% NaOH	1.22	1.29	0.39	0.04
4 mol% TMAH	1.08	1.30	0.31	0.28*
6.2 mol% TMAH	1.06	1.29	0.40	0.17
4 mol% Triton B	1.22	1.39	0.38	0.55*
6.7 mol% Triton B	1.24	1.37	0.47	0.57
4 mol% 50/50 NaOH/TMAH	1.08	1.35	0.24	0.26*
8 mol% 50/50 NaOH/TMAH	1.09	1.30	0.40	0.09
4 mol% 50/50 NaOH/TritonB	1.14	1.40	0.31	0.69*
8 mol% 50/50 NaOH/TritonB	1.23	1.37	0.47	0.61

As can be seen in Table 3.5, the highest α value was obtained for NaOH combined with Triton B. With regards to this, the solvatochromic parameters were also measured for different ratios of NaOH-to-TMAH and NaOH-to-Triton B (see Paper II [84]). From these measurements, it was clear that when NaOH was combined with Triton B, the parameters seemed to be dominated by the properties of Triton B, as shown in Figure 3.3. This shows that Triton B probably enriches in the shell around the dye, and therefore the dye does not reflect the properties of the bulk solvent. In the literature, this non-ideal behavior has been stated to be a common observation for Reichardt's dye (the α dye) in solvent mixtures [91].

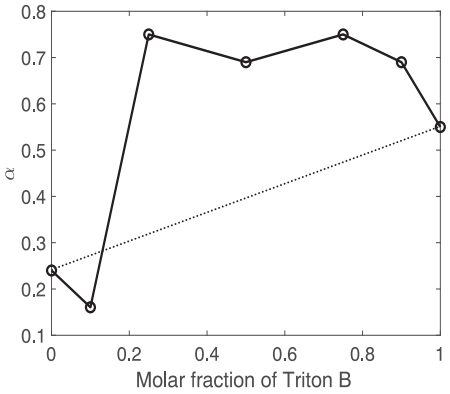

Figure 3.3: The Kamlet-Taft parameter α as a function of the molar fraction of Triton B in a 4 mol% NaOH/Triton B(aq). The dashed line illustrated ideal behaviour.

The solvatochromic parameters were also measured as a function of increasing temperature (see Table 3.7), however no significant effect of temperature could be discerned. In some cases there were also difficulties in determining α due to a weak signal from the dye.

Table 3.7: The Kamlet-Taft parameters of 4 mol% base(aq) as a function of increasing temperature.

T [°C]	π^*	β	α
-5	1.10	0.55	0.36
15	1.12	0.55	0.35
35	1.14	0.53	0.28
55	1.10	0.59	0.25
70	1.10	0.57	0.22

(a) NaOH

T [°C]	π^*	β	α
-5	1.08	0.61	0.38
15	1.01	0.71	0.43
35	1.08	0.61	0.35
55	1.08	0.63	-
70	1.06	0.65	-

(b) TMAH

T [°C]	π^*	β	α
-5	1.23	0.66	0.74
15	1.23	0.62	0.71
35	1.23	0.60	0.69
55	1.17	0.62	0.69
70	1.14	0.67	0.70

(c) Triton B

T [°C]	π^*	β	α
-5	1.18	0.52	-
15	1.16	0.55	0.34
35	1.14	0.57	0.25
55	1.14	0.59	0.30
70	1.14	0.59	-

(d) 50/50 NaOH/TMAH

T [°C]	π^*	β	α
-5	1.23	0.66	0.74
15	1.14	0.68	0.87
35	1.16	0.66	0.83
55	1.16	0.62	0.79
70	1.14	0.63	0.79

(e) 50/50 NaOH/Triton B

3.4 Is the cellulose ever molecularly dissolved?

As mentioned in the 'theory and background', solutions of polymers behave differently from solutions of low molecular weight compounds. Obtaining a transparent solution is certainly a sign of dissolution and simple visual inspection of the solution by eye or microscope is not an uncommon method to asses if the cellulose has dissolved or not. It does not however say whether the cellulose is molecularly dissolved or not. Thus, in order to investigate the size and conformation of the MCC in the different solvents, scattering methods were employed. Dynamic light scattering (DLS) was used to measure the effective hydrodynamic radius (R_h) of the cellulose in solution when dissolved at a dilute concentration. Static light scattering (SLS) was performed to measure the z-average radius of gyration ($R_{g,z}$) and the apparent weight average molecular weight (M_w). Finally, small angle X-ray scattering (SAXS) measurements were performed to provide information on the structure of the cellulose to complement the size information obtained from DLS and SLS. The measurements were performed at the lowest possible temperature for the respective instrumentation in order to hinder aggregation. An overview of the measurement conditions is presented in Table 3.8.

Table 3.8: Overview of the methods and measurement conditions.

Method	Concentration [g/ml]	Temperature
DLS	1×10^{-3}	20 °C
SLS	$5 \times 10^{-4} - 1 \times 10^{-2}$	7 °C
SAXS	1×10^{-2}	3 °C

As detailed in section 1.3 in the theory and background, the theoretical radius of gyration can be calculated in order to give an idea of what size one can expect from a molecularly dissolved cellulose. This was performed for the microcrystalline cellulose used in this thesis, and the contour lengths were based on the molecular weights obtained from GPC-MALS of MCC dissolved in DMAc/LiCl (see the chapter on materials and methods). The models used are those of of a Gaussian chain, a rigid rod and a worm-like chain. As can be seen in Table 3.9, the radius of gyration increases with increasing stiffness of the cellulose chain and in the order of number average < weight average < zeta average.

Table 3.9: Calculated theoretical number-, weight- and zeta average radius of gyration.

Model	$R_{g,n}[nm]$	$R_{g,w}[nm]$	$R_{g,z}[nm]$
Gaussian chain (b 1 AGU)	1.8	2.8	4.0
Cylinder (rigid rod) (d 0.5 nm)	11	27	53
Worm-like chain (l_p 4 AGU)	5	8	11
Worm-like chain (l_p 10 AGU)	7	12	18
Worm-like chain (l_p 20 AGU)	10	17	24
Worm-like chain (l_p 50 AGU)	12	24	37

For DLS the samples were measured both unfiltered and filtered with a 1.2 or 0.22 μm filter, in order to enable the detection of possible aggregation as well as molecularly dissolved cellulose chains. The normalised raw correlation curves are presented in Figure 3.5 and in order to calculate the effective hydrodynamic radius both a cumulant fit (see Table 3.10) and a multimodal distribution were applied (see Figure 3.4 and Paper III [92]). Firstly, it is clear, due to the effect on the correlation curves (Figure 3.5) and the decrease of the sizes obtained after a cumulant analysis (Table 3.10), that filtration with the two different filters had a large effect on the cellulose in NaOH(aq) and in NaOH/Triton B(aq). This shows that the cellulose was not well-dissolved, as a comparatively large portion of the sample was aggregated. This also shows that the combination of NaOH with Triton B did not improve the solution structure when compared to pure NaOH(aq). In fact already when the viscosities of the pure solvents were measured, the solvent of NaOH with Triton B(aq) showed slightly shear-thinning behaviour as opposed to the expected Newtonian behaviour which was observed for the other solvents. This indicates aggregation of the solvent itself. From the results on the dissolution capacity of cellulose dissolved in NaOH(aq) combined with Triton B(aq), it was clear that this combination did not improve the solvent quality. Instead it was a slightly poorer solvent than expected from the mere average of the two individual solvent bases. This indicates that even though NaOH and Triton are both soluble in water to a large extent, they might not be completely miscible, as the Triton base might be aggregating in the presence of NaOH. In fact, if one considers that Triton B is a weak surfactant it is likely to show self-aggregation behaviour, particularly at high ionic strength [93]. This could explain the observed solution properties and might also have contributed to the observation from the solvatochromic parameters on NaOH combined with Triton B: the dye did not reflect the bulk properties of the solvent.

The cellulose dissolved in TMAH(aq) and Triton(aq) was unaffected by filtration and well-dissolved as indicated by the small radii obtained from the cumulant analysis (Table 3.10). However, there was a feature in the correlation curves indicating two populations of cellulose. This was most distinct in the correlation curves of cellulose in Triton(aq) (Figure 3.5c). The multimodal distributions for the TMAH and Triton solutions showed that there is a high intensity scattering from the small-sized population of ca. 10 nm (Figure 3.4) and a fraction with a size of ca. 80-100 nm. As smaller particles scatter less light, the high intensity from the 10 nm population reflects that the majority of the cellulose in these samples was probably molecularly dissolved.

Table 3.10: Results from a cumulant analysis of the DLS data of cellulose in 4 mol% base(aq).

Solvent(aq)	Unfiltered $R_{h,z}$ $[nm]$	PDI	Filtered 1.2 μm $R_{h,z}$ $[nm]$	PDI	Filtered 0.22 μm $R_{h,z}$ $[nm]$	PDI
NaOH	81	0.81	48	0.99	28	0.62
TMAH	16	0.64	15	0.72	12	0.65
Triton B	9	0.96	10	0.93	11	0.95
50/50 NaOH/TMAH	32	0.91	27	0.95	21	0.61
50/50 NaOH/Triton B	120	0.91	36	0.61	8	1.0

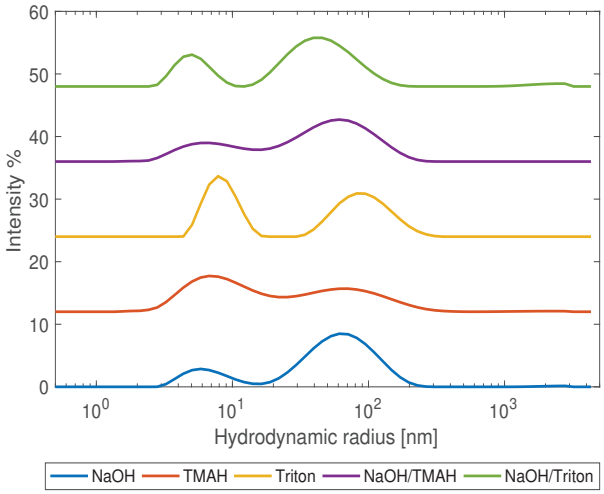

Figure 3.4: Size distributions of cellulose solutions filtered with a 0.22 μm filter, obtained through a multimodal fit. The curves are baseline shifted for improved readability.

When NaOH was combined with TMAH(aq) the cumulant analysis showed that the cellulose was more well-dissolved than in NaOH(aq), but larger than in TMAH(aq). Even though there was no sign of multiple populations in the correlation curves for NaOH/TMAH(aq) (Figure 3.5d), the PDI obtained from the cumulant analysis was high and the distribution fit indicated two populations with a radius of around 10 nm and 70 – 100 nm, respectively (see Figure 3.4).

While for this thesis, the DLS measurements were made on one dilute concentration, another extensive DLS study by Lu et al. on cellulose dissolved in NaOH/urea(aq) showed that upon increasing concentrations of cellulose, increasing temperature or increasing storage time, cellulose continued to aggregate further [94]. A similar behavior might be expected for the solvents used in this thesis, although the temperature stability might differ between the solvents.

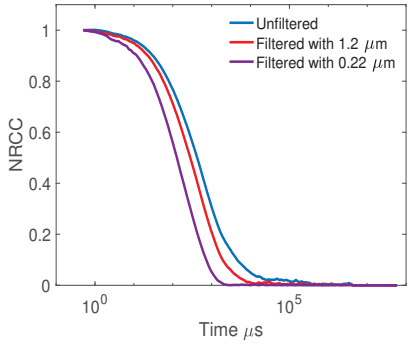

(a) NaOH

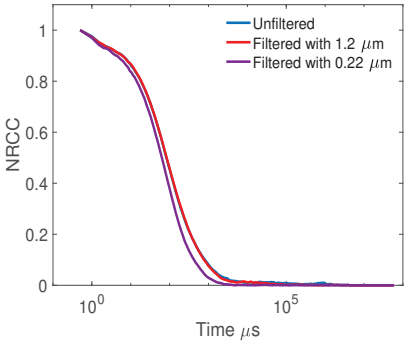

(b) TMAH

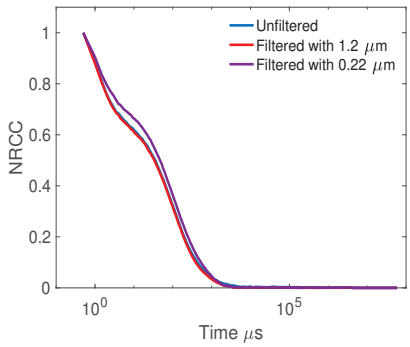

(c) Triton B

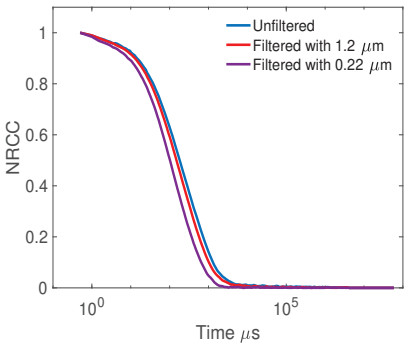

(d) 50/50 NaOH/TMAH

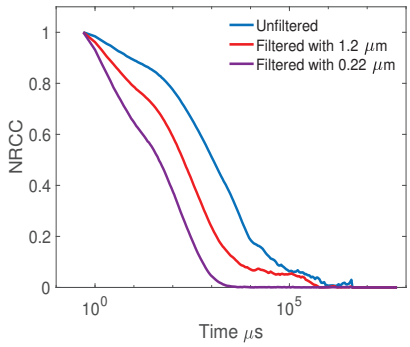

(e) 50/50 NaOH/Triton B

Figure 3.5: Normalised raw correlation coefficient (NRCC) as a function of time for MCC in the specified solvent.

For SLS a series of concentrations were measured in order to perform a Zimm-plot analysis of unfiltered and filtered solutions of dissolved cellulose. Since more concentrated samples were needed for SLS than for DLS it also became apparent that the Triton solutions were the easiest to filter, and the NaOH solutions the most difficult. Due to the difficulties of filtering the NaOH(aq) solutions with the 0.22 μm filter, only a partial Zimm-analysis on the lowest measured concentration (0.7×10^{-3} g/ml) could be performed for this sample. The results are seen in Table 3.11 and show large radii and high molecular weights for the unfiltered samples, indicating that there were aggregates in all of the solutions. However, the largest aggregates were found in NaOH(aq). If we compare the results on the molecular weights after filtration with a 0.2 μm filter, to the weight average molecular weight obtained from GPC-MALS in DMAc/LiCl, it appears that TMAH(aq) and Triton(aq) can dissolve part of the cellulose on a molecular level. If the obtained values of $R_{g,z}$ from the filtered samples are compared to the theoretically calculated ones, they indicate that the cellulose chains exist as stiff worm-like chains rather than gaussian chains. The combined solvents showed slightly better dissolution than NaOH(aq), but appeared to contain aggregates even after filtration with a 0.22 μm filter.

Table 3.11: Results from a Zimm-plot analysis on the data from the static light scattering measurements made on 4 mol% base(aq) solutions.

Solvent(aq)	Unfiltered $R_{g,z}$ [nm]	M_w [g/mol]	Filtered 0.22 μm $R_{g,z}$ [nm]	M_w [g/mol]
NaOH[2]	294	7.5×10^6	47	3.3×10^5
TMAH	173	2.4×10^6	24	4.5×10^4
Triton B	103	2.0×10^5	35	6.3×10^4
50/50 NaOH/TMAH	152	1.6×10^6	85	3.3×10^5
50/50 NaOH/Triton B	162	3.3×10^6	75	1.9×10^5

For the SAXS measurements, the concentration had to be increased above that which was used for DLS and SLS in order to get good statistics, and therefore the solutions were most likely in the semi-dilute state. The cellulose was thus influenced by interactions between cellulose chains and, based on the knowledge obtained from DLS and SLS, consisted of both dissolved and undissolved cellulose fractions of different aggregate sizes. Adding the fact that cellulose is inherently polydisperse, the difficulties of modelling these systems is further increased. Considering the presented difficulties, the power law behaviour was first fitted to provide information about the structure of the cellulose without assuming a model (see Figure 3.6). The fitted q-range was from 0.01 to 0.1 Å^{-1} (corresponding to a distance of 6.3 – 63 nm in real space). The results were an exponent of -1 for cellulose in Triton(aq) and TMAH(aq), which according to scattering theory suggests that at this length scale we are probing a stiff rod-like structure [95]. This indicates that in these two solvents the cellulose is closer to a stiffer worm-like chain than a fully flexible random coil, which also could indicate a strong association of the quaternary ammonium cations to cellulose. In regard to cellulose in NaOH(aq), the obtained exponent of -1.65 is typically associated with swollen chains in a good solvent [95]. However, since all other measurements indicate that it is indeed a

[2]Only a partial Zimm-plot analysis was performed for NaOH(aq) filtered with the 0.2 μm filter.

rather poor solvent, this could instead be interpreted as part of the cellulose being more flexible in NaOH(aq) than in Triton(aq) or TMAH(aq). For the combined solvents, the exponents of 1.35 for NaOH/TMAH and 1.4 for NaOH/Triton are close to the average between NaOH and TMAH (1.38) or NaOH and Triton (1.33). These values are more difficult to interpret, and reflect that the solutions' structure is somehow in between a more well-dissolved solution, as in TMAH(aq) or Triton(aq) and the aggregated state of NaOH(aq). It can both indicate that the two bases are distributed randomly along the chains (resulting in a semi-flexible chain), or that there is a mix of flexible and stiff chains.

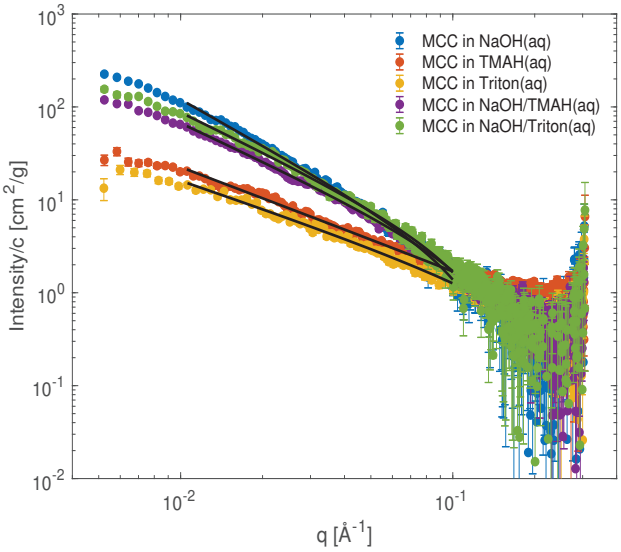

Figure 3.6: SAXS data normalised by concentration with the black lines showing the power law fitted to the q region in the range from 0.01 to 0.1 Å^{-1}.

The data was subsequently fitted using a model for a semiflexible polymer with excluded volume, where the fitting parameters were the contour length, Kuhn length (2 times the persistence length Lp for a worm-like chain) and the radius of the cellulose chain (see Figure 3.7, 3.8 and Table 3.12) [96]. This model does not take into account aggregation of the cellulose or polydispersity of the chains. The result obtained for cellulose in NaOH(aq) was a very long and flexible chain (see Table 3.12), reflecting what was already observed from the power law dependence.

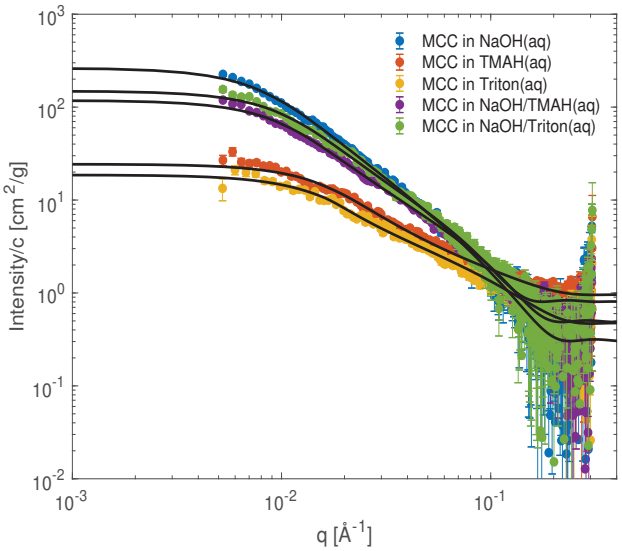

Figure 3.7: SAXS data together with black lines showing the fitted curves of the model for a semi-flexible worm-like chain.

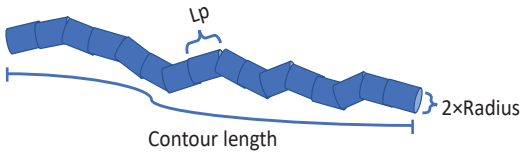

Figure 3.8: An illustration of a worm-like semi flexible cellulose chain and the fitted parameters.

The results for cellulose dissolved in TMAH(aq) or Triton(aq) reflect a stiffer and shorter chain than in NaOH(aq) as seen by the persistence and contour lengths (see Table 3.12). The contour lengths were shorter than expected since they correspond to a DP of ca. 120 and 85 for cellulose in TMAH and Triton. These values are closer to the number average DP than the weight average DP as measured by GPC-MALS (assuming that the length of an anhydroglucose unit is 0.515 nm) [97]. SAXS data should be closer to reflecting the weight average or zeta average since the intensity is proportional to the volume of the particle to the power of 6 and therefore the longer chains should scatter more. One explanation for a shorter chain length could be degradation of the cellulose chain but the samples were measured at close to 0 °C and so no degradation is expected. The obtained radius of the chain is larger than expected for a single cellulose chain (within the order of 2 Å, not including the counter ion). Therefore, another explanation for the short contour length might be that the chain is taking a longer path inside the flexible cylinder that the model is representing, and so the true contour length might be longer. For the two combined solvents the results of applying the model for the semi-flexible chain are very similar to each other: they both return a contour length corresponding to a DP of ca. 235, persistence lengths of ca. 4.5 nm and radii in line with that obtained for the other solutions (see Table 3.12). In general, the findings show that the cellulose is stiffer in Triton(aq) and TMAH(aq) than in NaOH(aq), which could be a result of the cellulose being more well-dissolved in TMAH(aq) and Triton(aq).

Table 3.12: Results from the fitting of the model to the SAXS data.

	NaOH	TMAH	Triton B	50/50 NaOH/TMAH	50/50 NaOH/Triton B
Contour length L [nm]	356 ± 88	62 ± 2	43 ± 2	118 ± 2	121 ± 4
Kuhn length l_k [nm]	3.2 ± 1.1	7.7 ± 0.5	19 ± 1.0	9.5 ± 0.3	8.6 ± 0.5
Persistence length l_p [nm]	1.6	3.6	9.4	4.8	4.3
Chain radius [Å]	16 ± 1.0	12 ± 0.1	13 ± 0.4	18 ± 0.2	22 ± 0.4

3.5 Rheology of the solutions

In order to investigate the effect that the different bases had on the properties of the cellulose solutions, rheological measurements were made and the stability of the solutions was measured over time and against an increase in temperature.

Flow sweeps of solutions without urea

The viscosity of the samples was measured as a function of the shear rate in so-called flow sweeps of samples with 3 wt.% MCC in 2 M base(aq) solutions, details are found in Paper III [84]. For a solution without entanglements (and below the overlap concentration), a fully Newtonian behaviour would be observed, where the viscosity is independent of the shear rate. The flow sweeps showed that at the investigated cellulose concentration, the NaOH(aq) solution was never fully Newtonian (see Figure 3.9a), indicating that there were entanglements in the solution and that 3 wt.% cellulose was above the overlap concentration. At 45 °C the viscosity at low shear rates increased substantially, which is possibly due to further aggregation and partial precipitation of cellulose. This indicates that the cellulose in NaOH(aq) is not stable against elevated temperatures. This is in line with the observations on the solution structure of cellulose in NaOH(aq) from the scattering methods, showing that NaOH(aq) is a rather poor solvent. The TMAH(aq) solution exhibited mostly Newtonian behaviour over the investigated temperature interval (Figure 3.9b)), indicating a higher temperature stability than for cellulose in NaOH(aq) solution.

Combining NaOH and TMAH resulted in a solution that became shear thinning with increasing temperature (Figure 3.9d). Shear thinning commonly indicates the formation of a polymer network and could, in this case, indicate that the overlap concentration had decreased with an increase in temperature.

The Triton B(aq) solution displayed completely Newtonian behaviour regardless of the applied temperature (see Figure 3.9c), indicating a greater temperature stability than NaOH(aq), in line with the observations by Wang et al. [66]. When combining NaOH with Triton B (Figure 3.9e), the flow properties deteriorated with increasing temperature as shear thinning could be observed. The flow behaviour was still better than what was found for NaOH(aq) alone, but worse than that of the NaOH/TMAH combination. This aligns with the findings for dissolution capacity and solution structure, showing that the properties are reflected in the solution structure.

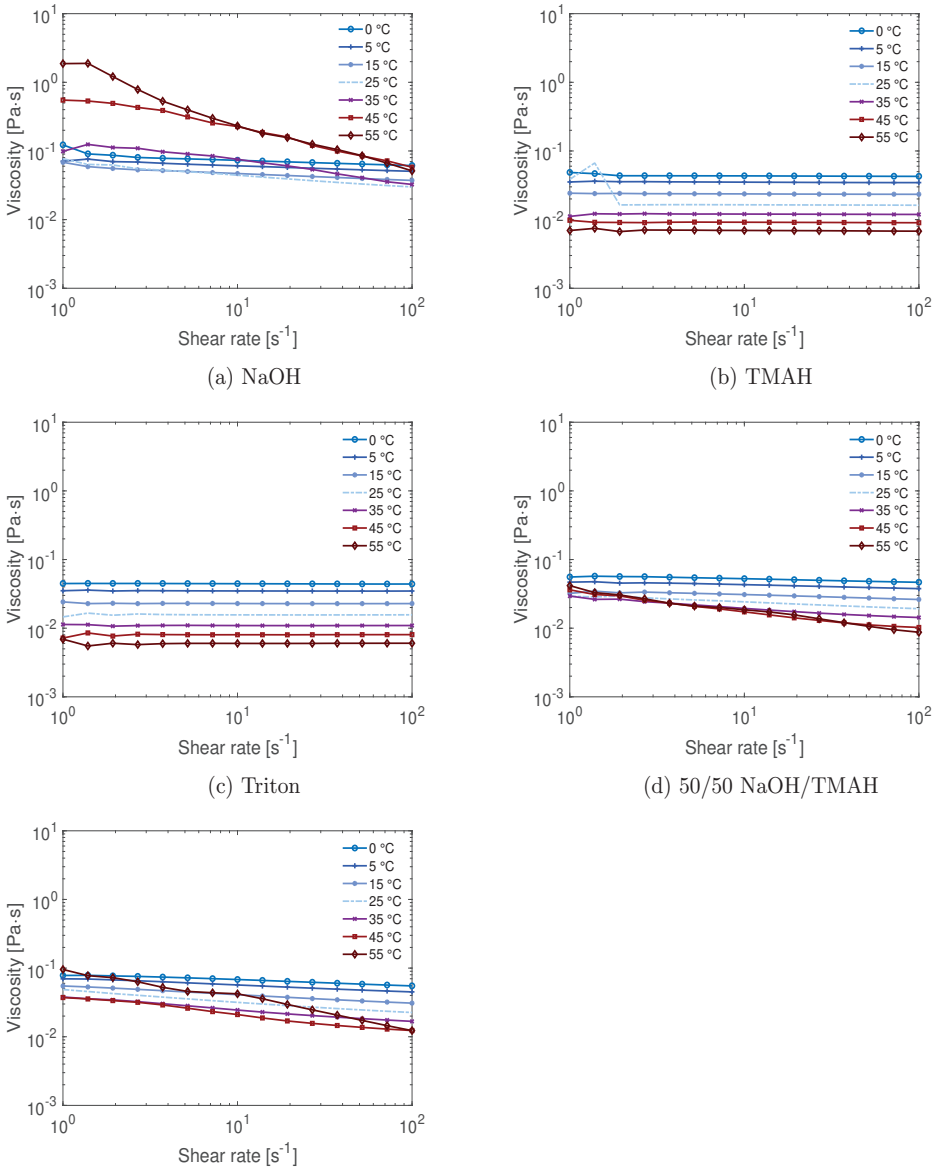

(a) NaOH

(b) TMAH

(c) Triton

(d) 50/50 NaOH/TMAH

(e) 50/50 NaOH/Triton

Figure 3.9: Flow sweeps of ca. 3 wt% MCC in 4 mol% base (11:1:266 molar ratio of base:AGU:H_2O).

Flow sweeps of solutions with urea

The flow sweeps of the solutions that also contained urea showed similar trends as the results from the dissolution capacity measurements. The addition of urea enhanced the Newtonian behaviour of solutions containing NaOH and/or TMAH (Figure 3.10a, 3.10d and 3.10b), but did not have the same effect on solutions with Triton B (Figure 3.10c). This is also demonstrated by the fact that the NaOH/TMAH/urea solution (Figure 3.10d) displayed Newtonian behaviour over the entire temperature range, in contrast to the same solution without urea (Figure 3.9d).

The addition of urea to Triton B(aq)(Figure 3.10c) had no impact on the flow sweeps of the solution, but it is difficult to draw any conclusions based solely on this since the Triton B solution was fully Newtonian even without urea. On the other hand, the NaOH/Triton B/urea solution (Figure 3.10e) was less shear thinning than the corresponding solution without urea, but not fully Newtonian like the Triton B solutions. This is in line with the results on dissolution capacity, and indicates that the addition of urea probably improves the dissolution capacity and dissolution properties of NaOH(aq), but not Triton B(aq).

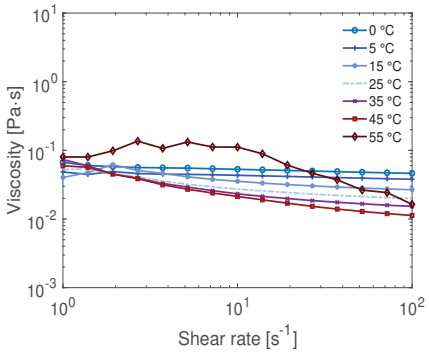

(a) NaOH+urea

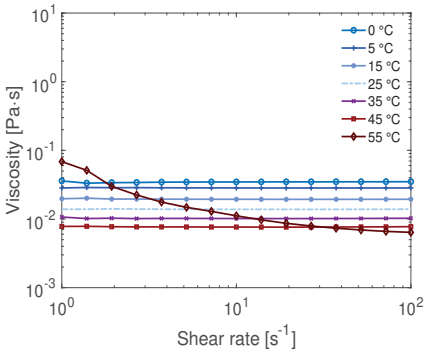

(b) TMAH+urea

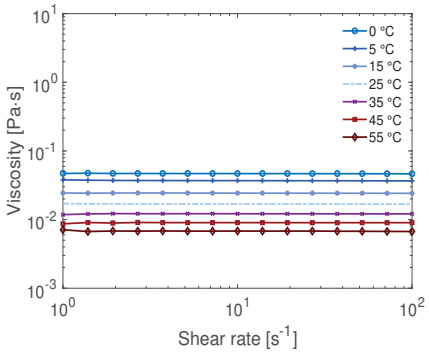

(c) Triton+urea

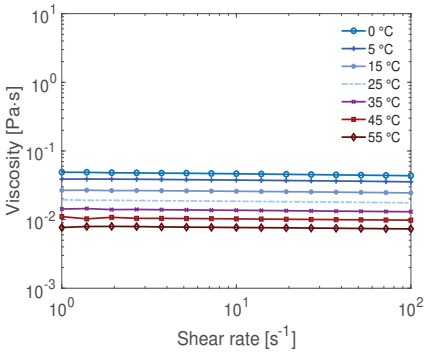

(d) 50/50 NaOH/TMAH+urea

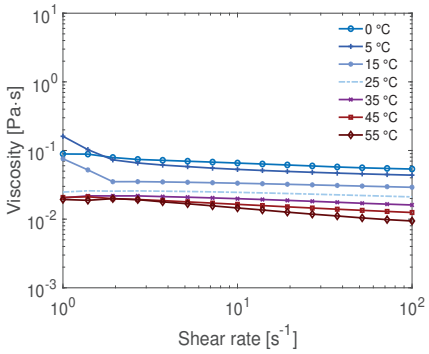

(e) 50/50 NaOH/Triton+urea

Figure 3.10: Flow sweeps of ca. 3 wt% MCC in 3.8 mol% base and 4.4 mol% urea (11:1:266:13 molar ratio of base:AGU:H_2O:urea).

3.6 A closer look at cellulose in 50/50 NaOH/TMAH(aq)

From the measurements on dissolution capacity and the size of cellulose in solution, it was apparent that combining NaOH with TMAH resulted in better properties than combining NaOH with Triton B, due to the miscibility issues. Therefore, the following section will focus on cellulose dissolved in NaOH/TMAH(aq). Between NaOH(aq) and TMAH(aq), the difference in molar volume was not as significant as between for example NaOH(aq) and Triton B(aq). Therefore Molar is used instead of mol% in this section.

At what temperature can MCC be dissolved?

In order to study if combining NaOH with TMAH had any influence on the temperature at which dissolution occurred, and to measure more precisely what temperatures were required, the temperature dependency of dissolution was measured. The solvent was set to the desired temperature before the cellulose was added, and the cellulose concentration was kept low to facilitate dissolution (ca. 1 wt.%). The transmission of the solution was then measured as an indication of dissolution (see Paper IV for details). The results for the cellulose in the three solvents, NaOH(aq), TMAH(aq) and 50/50 NaOH/TMAH(aq), showed that the regions in which dissolution occurred were quite similar. The transmission never reached 100 % for cellulose in NaOH(aq), which is in line with the findings from the scattering measurements, that even at low concentrations of MCC there are undissolved fibres remaining in solution [92]. Despite this, the temperature window in which the transmission was close to 100 %, and dissolution to some degree occurred, expanded for all three solvents with increasing base concentration of up to ca. 2 M (see Figure 3.11a-c), which was the optimum (Figure 3.11c). When going above 2 M, the temperature window decreased again (Figure 3.11d-e). For all three solvents, at concentrations of 1.5 - 2 M, the temperature dependency of dissolution was very strong as can be seen from the steep drop in transmission (see Figure 3.11a-c). The exact temperature at which this sudden drop occurred cannot be distinguished with significance between the three solvents, rather they display very similar results. At and above 2.5 M (Figure 3.11e-f), the difference between the solvents was larger, and we can state that NaOH retains its ability to dissolve cellulose at low temperatures and is a significantly better swelling agent than TMAH. As for the combined solvent, the temperature dependency seems to correspond roughly to an average of the two up until 2.75 M, at which it has a lower swelling capacity than TMAH (Figure 3.11f). This possibly indicates that the base combination loses its dissolution ability when one of the bases does.

This study also emphasises that, although dissolution through a protocol based on freezing and thawing is commonly reported in literature (for example [58][98]), freezing is not a requirement for MCC, but achieving low temperatures is crucial for dissolution to occur. It is possible however, that freezing is more important for fibrous celluloses where more of the native hierarchical structure remains, as it could influence the microstructure of the cellulose due to the expansion of ice.

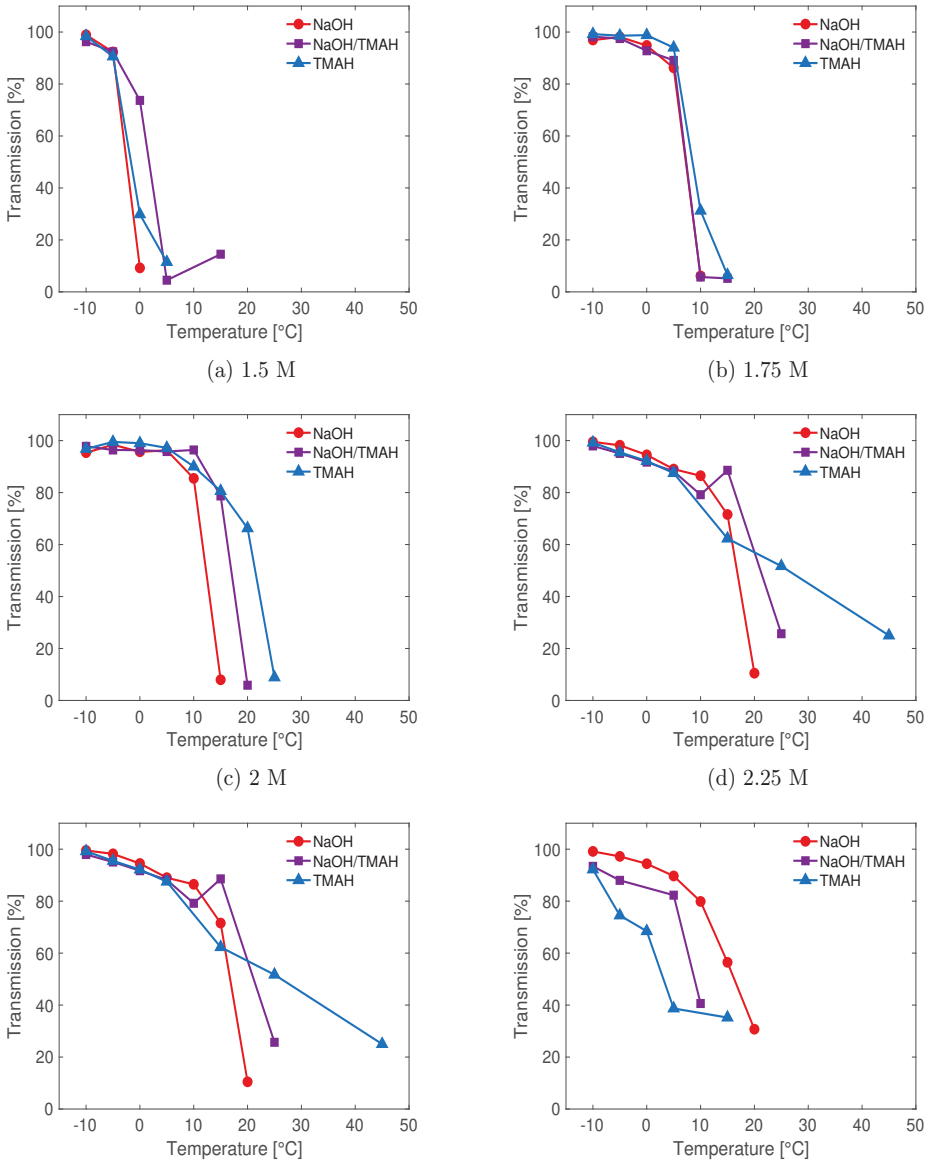

(a) 1.5 M

(b) 1.75 M

(c) 2 M

(d) 2.25 M

(e) 2.5 M

(f) 2.75 M

Figure 3.11: Transmission as a function of temperature of the solvent for 10 g cellulose/L (ca. 1 wt%) at the specified base concentration.

Structure of the base hydrates in the solvents

Additionally, thermoscans were performed using DSC to identify melting temperatures and enthalpies of different hydrates in the solutions in order to investigate the structure of the hydrated bases and to study their interactions with cellulose. For NaOH concentrations around 2 M(aq), Roy et al. have reported that a eutectic hydrate salt with a composition of NaOH·9 H_2O (melting temperature T_m of - 34 °C) and unbound water are present in solution [99]. The same could be identified here (solvent ratio of 100/0 NaOH/TMAH in Table 3.13). Thermoscans of 2 M(aq) TMAH(aq) solution have shown that it contained a eutectic hydrate salt with a T_m of -26.3 °C and unbound water, as seen in Table 3.13. This is in agreement with a previously reported investigation of TMAH hydrates: from the published phase diagram by Mootz and Siedel the structure of the eutectic hydrate salt can be calculated to TMAH·16 H_2O and the T_m read from a diagram as -28 °C [100]. The ratio of the bases was then varied in order to observe how the hydrates of NaOH and TMAH would be affected by each other. In a solution of 75/25 mol% NaOH/TMAH(aq), it seems that hydrates were formed with the same structures as in the reference solutions of pure NaOH(aq) and pure TMAH(aq), based on the fact that there was no significant shift in their melting temperatures. The enthalpy of the NaOH hydrate, however, decreased significantly, indicating only a modest crystallization of the previously observed NaOH hydrates. When the concentration of TMAH was increased further to a ratio of 50/50 NaOH/TMAH(aq), two hydrate salts were observed with melting temperatures close to each other. Based on the enthalpies, the hydrate with a T_m of $-$ 27.8 °C was attributed to NaOH and the other with a T_m of -25 °C to the TMAH hydrate. For the NaOH hydrate the melting point was now closer to that reported for NaOH·7 H_2O than for NaOH·9 H_2O [101]. When the concentration of TMAH was increased even further to a ratio of 25/75 NaOH/TMAH(aq), only one peak (besides that of ice) was observed, with a melting temperature and enthalpy consistent with a TMAH salt. It is reasonable to assume that NaOH was still hydrated by water and present in the solutions even when there was no identifiable peak in the DSC trace. However, these measurements show that the presence of TMAH can prevent the NaOH hydrate from crystallising. The same behaviour had previously been observed by Egal et al. upon dissolution of MCC in NaOH(aq) [102]. The TMAH hydrate probably retains its structure, with its melting temperature affected only slightly by a change in solution composition.

Table 3.13: Melting temperature T_m [°C] and enthalpy ΔH [J/g sample] of peaks in 2 M(aq) base solutions.

Solvent ratio	T_m °C NaOH	ΔH [J/g] NaOH	T_m °C TMAH	ΔH [J/g] TMAH	T_m °C Ice	ΔH [J/g] Ice
100/0 NaOH/TMAH	-33.7	95.0	-	-	-9.7	170.6
75/25 NaOH/TMAH	-34.4	16.1	-25.3	41.5	-13.2	30.6
50/50 NaOH/TMAH	-27.8	15.3	-25.1	72.2	-14.7	42.1
25/75 NaOH/TMAH	-	-	-27.3	69.4	-16.0	41.9
0/100 NaOH/TMAH	-	-	-26.3	68.0	-17.3	27.8

Hydrate interaction with cellulose

It was observed that when cellulose was dissolved in the NaOH(aq) solution, the melting temperature of the NaOH hydrate decreased slightly and the enthalpy decreased significantly, as can be seen in Table 3.14, and as reported by Egal et al. [102]. Upon dissolution of cellulose in 2 M(aq) TMAH(aq), the same hydrate structure was formed as in the cellulose-free solutions, with only a slight decrease of the enthalpy of the TMAH hydrate. Upon dissolution of cellulose in the combined solvent, there was no major shift in the melting temperatures, indicating that the hydrate structures were also the same as in the cellulose-free solution, but a slightly larger decrease of the TMAH hydrate was observed. Thereafter, a series with increasing concentrations of MCC in 2 M(aq) 50/50 NaOH/TMAH(aq) was measured in order to further investigate how the base interacts with the cellulose. As can be seen in Figure 3.12, the enthalpy of the hydrate salt of TMAH decreased linearly with increased concentration of MCC, whereas the enthalpy of the hydrate salt of NaOH slightly increased. The implication is that TMAH interacts with the cellulose instead of forming a crystalline hydrate salt in the solution. However, the continuous decrease of the TMAH hydrate might not show that cellulose preferably interacts with TMAH, but that since the NaOH hydrates have not crystallized, their interaction cannot be followed by means of this method.

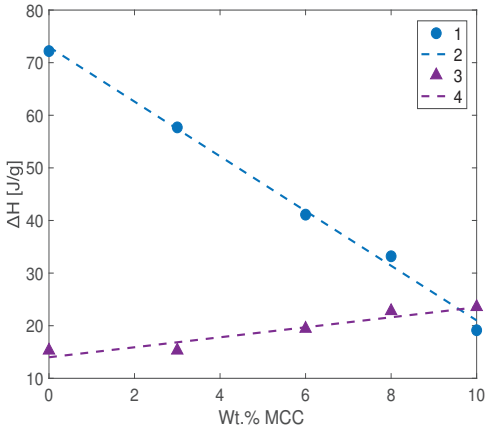

Figure 3.12: Enthalpy of TMAH-hydrate (1) with linear trendline (2) and NaOH-hydrate (3) with linear trendline (4) as a function of cellulose concentration in solutions of 2 M 50/50 NaOH/TMAH(aq).

In regard to the hydrated structures, it is interesting to note that the loss in dissolution ability of TMAH seems to coincide with the decrease of the unbound water. This is seen in the phase diagram of TMAH in water reported by Mootz and Seidel, when starting from the water-rich region and moving towards the eutectic point at ca 95 mol% water (corresponding to ca 2.75 M TMAH(aq))[100]. The same can be observed in the phase diagram of NaOH and water [28]. As shown through DSC, the water in the solvents are subject to freezing point depression. Supercooled water becomes less dense with decreasing temperature [103], assuming this is true for the water in these solvents, it might have a similar effect to actual freezing of water, i.e. to open up the cellulose structure. With this reasoning however, increasing temperature should also benefit dissolution since

it also decreases water density. This is not the case in 2 M(aq) base solutions, and one explanation might be that increasing temperatures does not benefit hydrogen bonding between the base/water and cellulose (or water to water) [52], while attractive dispersion forces between cellulose chains should be less affected by temperature.

Table 3.14: Melting temperature T_m [°C] and enthalpy ΔH [J/g sample] of peaks in 3 wt.% MCC solutions dissolved in 2 M(aq) base solutions.

Solvent ratio	T_m °C NaOH	ΔH [J/g] NaOH	T_m °C TMAH	ΔH [J/g] TMAH	T_m °C Ice	ΔH [J/g] Ice
100/0 NaOH/TMAH	-34.5	13.7	-	-	-9.0	68.7
50/50 NaOH/TMAH	-28.16	15.3	-25.4	57.7	-12.7	50.6
0/100 NaOH/TMAH	-	-	-26.4	63.2	-15.6	34.3

Interactions between the solvents and a model cellulose substrate

NMR analysis of a model cellulose substrate was performed in order to shed light on molecular interactions in the solutions. Replacing NaOH(aq) with TMAH(aq) led to a downfield displacement of all the ^{1}H chemical shifts observed. For the signal originating from water, a displacement in the chemical shifts corresponding to 0.15 ppm downfield could be observed upon replacement of 50% NaOH and, finally, displacement corresponding to additional 0.1 ppm when dissolved in TMAH only, as can be seen in Figure 3.13. It might be an effect of the perturbation of the water structure in close proximity to TMAH, causing the water structure to have lower mobility. ^{1}H chemical shifts of the model glucose compound are also displaced downfield; this is indicative of the displacement of electron density away from the glucose C–H protons and is possibly due to the proximity of the TMAH cation.

Furthermore, changes in ^{13}C chemical shifts (see Figure 3.14), albeit modest, additionally witness of perturbation of electron density experienced by the glucose ring upon addition of TMAH in the NaOH(aq) system. Carbon atoms in positions 2, 4 and 6 show deshielding effects when the amount of TMAH is increased (displacement of the chemical shift downfield corresponding to 0.2 ppm when going from NaOH(aq) to TMAH(aq)), while those in positions 1, 3 and 5 seem to experience a very poor shielding effect (a modest chemical shift displacement upfield).

Interestingly enough, this does not comply with the deprotonation signature commonly observed: an upfield displacement of ^{1}H chemical shifts together with a downfield displacement of the ^{13}C signals originating from the C atoms carrying deprotonable hydroxyl groups. Consequently, the presence of TMAH is probably not associated with enhanced deprotonation of the carbohydrate, it is more likely involved in other interactions responsible for deshielding of the glucose C–H moieties.

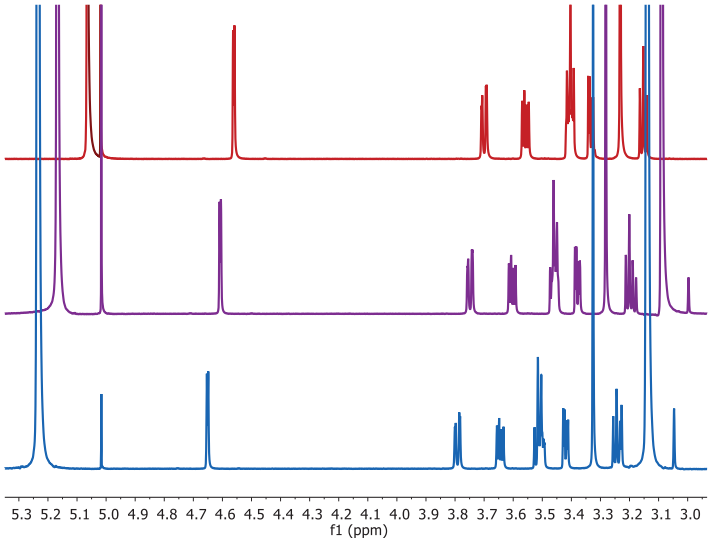

Figure 3.13: H-NMR spectra of methyl-α-D-glucopyranoside dissolved in 2 M NaOH (red spectra), 2 M 50/50 NaOH/TMAH (purple spectra) and 2 M TMAH (blue spectra), all in D_2O.

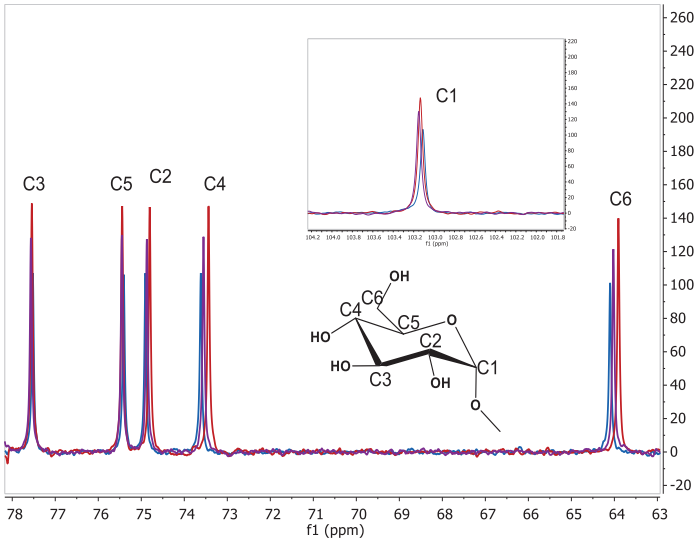

Figure 3.14: ^{13}C-NMR spectra of methyl-α-D-glucopyranoside dissolved in 2 M NaOH (red spectra), 2 M 50/50 NaOH/TMAH (purple spectra) and 2 M TMAH (blue spectra), all in D_2O.

Stability of cellulosic solutions over time and against an increase in temperature

From the study on the temperature of dissolution, the optimum dissolution conditions were 2 M base(aq) at ca. - 5 °C for all three solvents. The question therefore was if there is a difference in temperature stability of the dissolved cellulose, depending on the solvent. Cellulose was therefore dissolved under optimum conditions, and the temperature stability was measured at two different concentrations: 10 g/L (ca. 1 wt.%) (Figure 3.15a) and 30 g/L (ca. 3 wt.%)(Figure 3.15b).

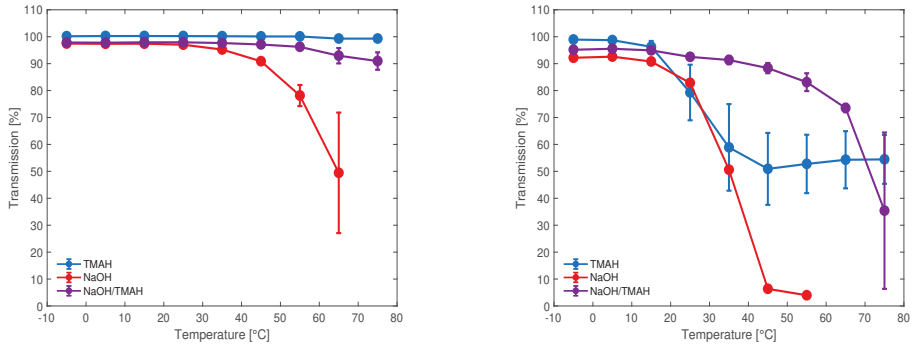

(a) 10 g cellulose/L

(b) 30 g cellulose/L

Figure 3.15: Transmission of solutions upon increasing temperature.

For 10 g/L, the cellulose in the NaOH aqueous solution became unstable above 35 °C, where the cellulose presumably started to aggregate and precipitate. The cellulose in the TMAH(aq) remained stable over the entire temperature interval measured (up to 75 °C), while the cellulose in the 50/50 NaOH/TMAH(aq) solution started to show aggregation/precipitation above 55 °C. For 30 g/L the temperature stability had decreased compared to 10 g/L for all three solvents. The 50/50 NaOH/TMAH(aq) solution gradually deteriorated with increasing temperature, but showed a better resistance towards increasing temperature than NaOH(aq) or even TMAH(aq). The difference in the observed results between the 10 g/L and 30 g/L might be explained if it is considered that the solutions were in different concentration regimes. The overlap concentration (approximated by the inverse of the intrinsic viscosity, see Paper I) should be around 10 g/L for all three solvents. Under the overlap concentration, the cellulose should not aggregate unless the solvent quality is deteriorating with increasing temperature. The latter is probably the case for 10 g MCC/L in NaOH(aq), that the solvent quality deteriorates due to the lack of a hydrophobic character while hydrogen bonding interactions weaken with increasing temperature, as also pointed out by others [52]. At 30 g/L, also a large difference in the transmission drop between NaOH and TMAH could be observed at elevated temperatures (Figure 3.15b), indicating that in NaOH(aq) the precipitated material was crystalline (which scatters more) while in TMAH(aq) a higher transmission was retained, indicating aggregated but less ordered cellulose.

The effect of combining NaOH with TMAH on the stability of the solutions over time has also been measured at different temperatures. This was done both with rheology measurements by monitoring the evolution of the loss and storage modulus over time (see Paper I), and in another experiment by following the transmission (see Paper IV). The rheological measurements monitored the gelation, since when the loss modulus is higher than the storage modulus the solution is more liquid-like. However, as the storage modulus increases and becomes higher than the loss modulus, this is a sign that the solutions have gelled or precipitated. As can be seen in Figure 3.16, the 50/50 NaOH/TMAH(aq) solution was more stable over time at all of the investigated temperatures (15, 25 and 35 °C). However, gelation eventually occurred for all the solutions, and faster with increasing temperature. The same trends were also found for more dilute cellulose solutions, containing less cellulose (see the supporting info to Paper I [83]). The results when measuring the stability of the solutions over time through transmission measurements confirmed these observations, as the 50/50 NaOH/TMAH(aq) solution was more stable over prolonged storage times at all of the investigated temperatures (8, 20 and 35 °C, Figure 3.17). This shows that combining NaOH with TMAH could somehow improve the stability of the solutions and delay the gelation.

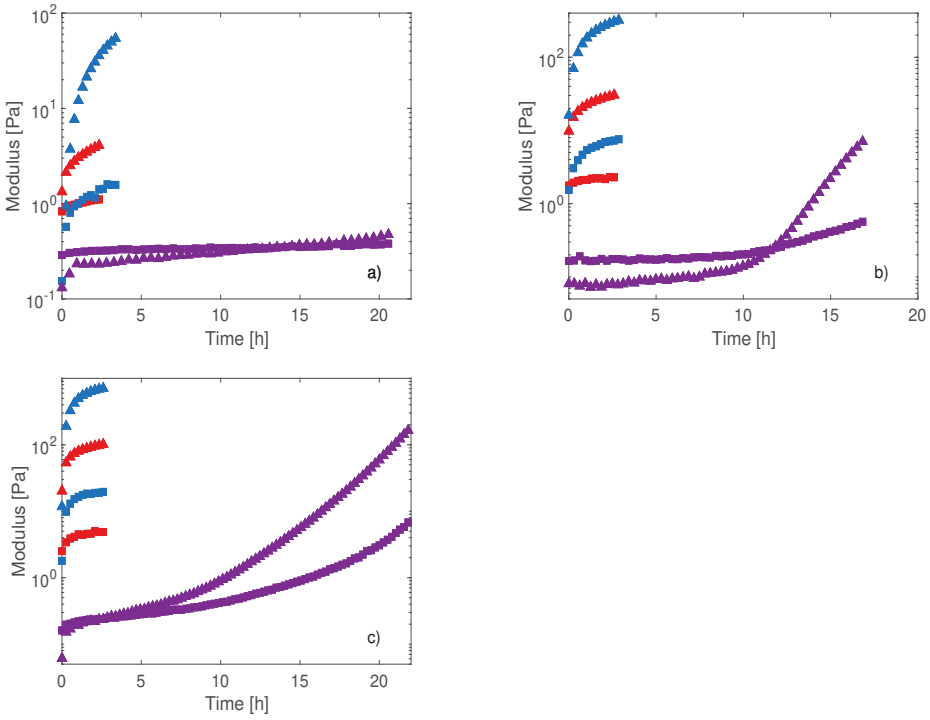

Figure 3.16: Storage modulus G'(triangles) and loss modulus G"(squares) of 5 wt% MCC in ca. 2 M NaOH(aq) (red), 2 M TMAH(aq) (blue) and 2 M 50/50 NaOH/TMAH(aq) (purple) as a function of time at a) 15 °C, b) 25 °C and c) 35 °C.

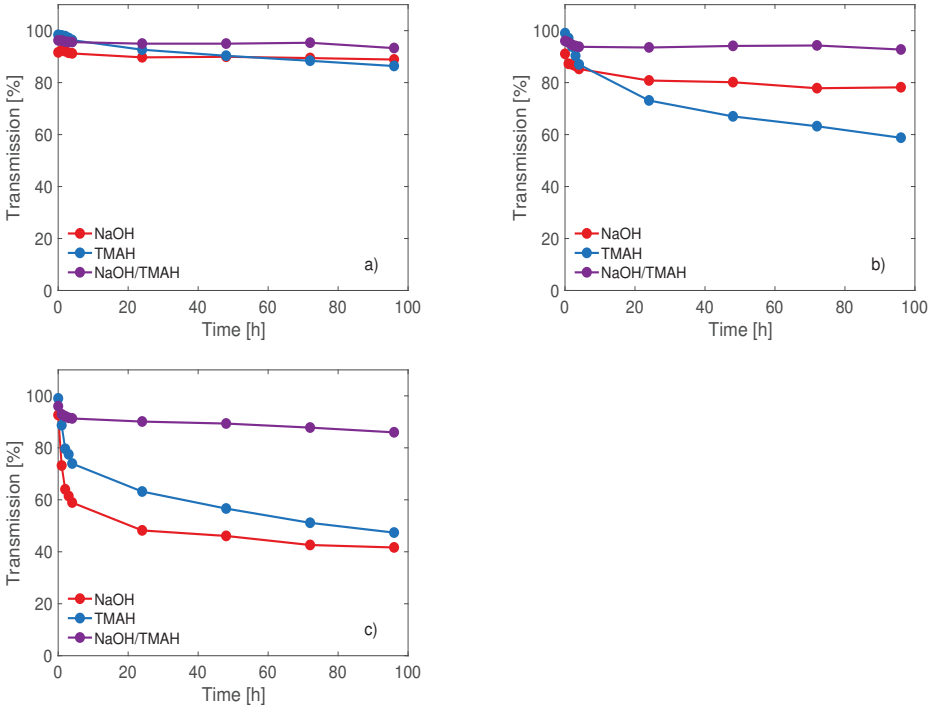

Figure 3.17: Transmission over time of cellulose (10 g/L) dissolved at – 5 °C in 2 M (aq) base solutions when stored at a) 8 °C, b) room temperature 20 °C and c) 35 °C.

Another observation that was made upon performing the stability measurements, was a color change of the solutions, increasing with temperature and storage time. The solutions went from colorless to a range of yellow or brown/black, which did not occur to the pure solvents. The color was most intensive for cellulose in TMAH(aq), followed by the combination and weakest for cellulose in NaOH(aq), and it mainly disappeared if the solutions were titrated with hydrochloric acid to acidic conditions.

Possible degradation of the cellulose

The observed color change warranted an investigation into possible degradation of the cellulose in the solutions. No reports in literature on coloring of cellulose dissolved in aqueous hydroxide solutions could be found, but for undissolved cellulose under alkaline conditions, it is documented that degradation occurs by peeling from the reducing ends, releasing glucose units one by one and forming different acids as degradation products. One study reports that the main degradation products of undissolved cellulose in 0.5 M NaOH(aq), after 720 days at 20 °C were D-glucoisosaccharinic acid, 3,4-dihydroxybutyric acid, 2-hydroxyacetic(glycolic) acid and formic acid [104]. These acids might also occur in these solutions and could be the source of the color when deprotonated in their sodium form. Although these degradation products are unwanted and might cause a problem for certain applications, it was important to measure if there was a significant decrease of the molecular weight of the cellulose. Therefore, the molecular weight distribution of the MCC after dissolution in 2 M base(aq) at – 5 °C and 30 g/L, and subsequent storage at 35 °C for 3 days was measured through size exclusion chromatography of samples dissolved in DMAc/LiCl, and compared to the MCC starting material. The measurements showed that there was no significant degradation of the cellulose, despite the coloring of the solutions. As seen in Figure 3.18, there was a small decrease in the low molecular weight fraction, which could be the fraction that is most subjected to peeling. It can be noted that the appearance of a high molecular weight fraction in cellulose that was previously dissolved in TMAH(aq) is probably due to aggregation in the DMAc/LiCl. The values obtained for the molecular weight averages can be found in paper IV.

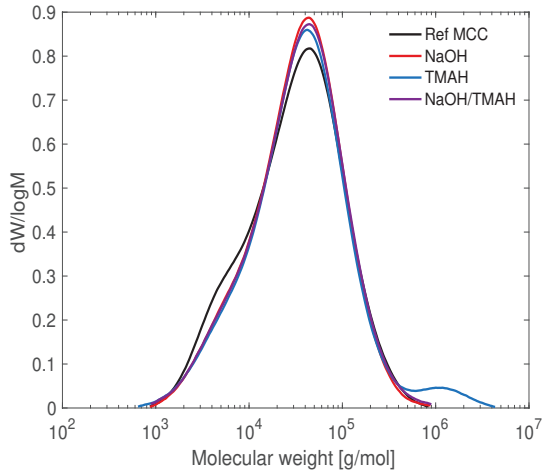

Figure 3.18: Molecular weight distribution of the MCC before (Ref MCC) and after dissolution in the specified solvent.

The crystalline structure before and after dissolution

The transformation from cellulose I to cellulose II in all three solvents after dissolution, coagulation, washing and drying of the MCC was confirmed through X-ray diffraction (see Figure 3.19). The identified peaks are listed in Table 3.15. The crystallinity index of the coagulated cellulose was calculated through the Segal method, but showed no large differences between the solvents (see Paper IV and Table 3.15).

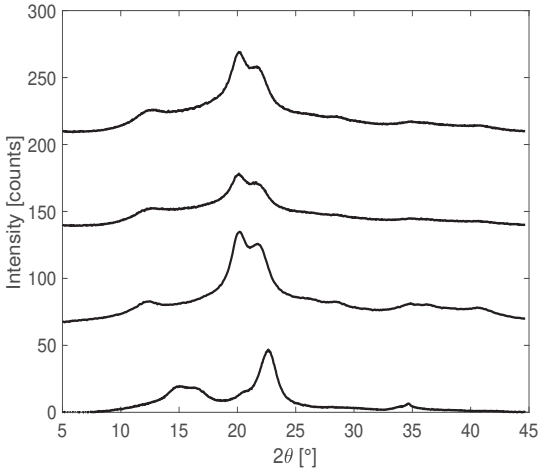

Figure 3.19: Starting from the bottom: X-ray diffraction of the starting material MCC and the coagulated MCC after dissolution in NaOH(aq), TMAH(aq) and 50/50 NaOH/TMAH(aq). The curves have been background subtracted and baseline shifted for improved visibility.

Table 3.15: Identified peaks and Segal crystallinity index (Cryst.I) of the MCC before (CI) and after coagulation in the respective solvents (CII).

	CI	CII NaOH	CII TMAH	CII NaOH/TMAH
Peak 1	15.2°	12.4°	12.8°	12.8°
Peak 2	16.7°	20.2°	20.1°	20.2°
Peak 3	20.8°	21.7°	21.5°	21.5°
Peak 4	22.9°	28.3°	28.3°	28.5°
Peak 5	34.6°	35.0°	35.4°	34.8°
Cryst.I	70 %	78 %	58 %	64 %

Intracrystalline swelling of the cellulose

In a fully dissolved cellulose sample there is no crystalline structure, but in order to mimic and investigate what occurs with the crystalline structure in different stages pre- and post dissolution, cellulose was soaked in the respective solvents and measured with X-ray diffraction at room temperature, and after storage at + 3 °C and – 20 °C. The sample was overloaded with cellulose to provide a measurable cellulose signal. Soaking at room temperature (see Paper IV), or even at + 3 °C for 22 h (Figure 3.20a) did not change the crystalline structure, as it remained as cellulose I. After storage at – 20 °C for 3 h, upon which the samples froze, the base had penetrated the crystal structure and altered it (see Figure 3.20b). Similar observations, that low temperatures are required before intracrystalline swelling occurs, have been recently reported for cellulose immersed in sulfuric acid [105]. The diffraction angles for the identified peaks of the swollen samples can be found in Table 3.16, along with the main peaks measured for cellulose I and cellulose II. None of the swollen samples corresponded completely to cellulose I or cellulose II, and all three samples showed different patterns. For cellulose soaked in TMAH(aq), there were however similarities to cellulose II, as the peaks at 20.65°and 21.66°are similar to those usually found at 20.5°and 21.9°, attributed to the (110) and (020) planes, when named as by Nam et al. [106]. In addition, a shoulder peak could be observed at 5.4°, similar to the observations made by Sisson and Saner, who measured the swelling of ramie fibres in TMAH(aq) at room temperature. For TMAH it was reported that the (101) plane ((1-10) when named as by Nam et al.) had an interplanar distance of 13 Å, which would correspond to a peak at ca. 7°, similar to the shoulder peak observed here [65].

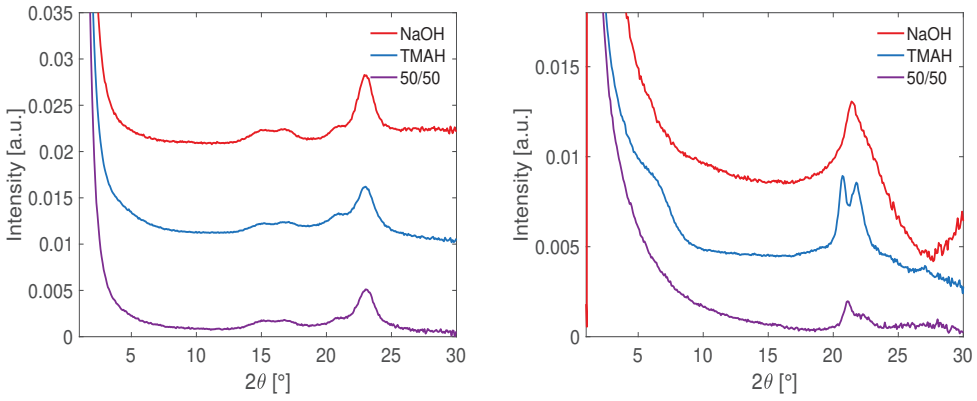

(a) Fridge, + 3 °C for 22 h

(b) Freezer, - 20 °C for 3 h

Figure 3.20: X-ray diffraction of MCC soaked in 1.75 M(aq) base, background of solvent and capillary subtracted and the curves have been baseline shifted for improved visibility.

Table 3.16: Identified peaks of MCC soaked in 1.75 M(aq) base, stored at - 20 °C for 3 h. Peaks obtained from the starting material (CI) and the average of those obtained for cellulose II (CII) given as a reference.

CI	CII	MCC NaOH	MCC TMAH	MCC NaOH/TMAH
-	-	-	5.4°	-
15.2°	-	-	-	-
16.7°	12.7°	-	-	-
20.8°	20.2°	-	20.7°	-
-	21.6°	21.5°	21.7°	21.1°
22.9°	-	-	-	22.3°

For MCC soaked in NaOH(aq), only one peak could be viewed, although from its appearance it might be deconvoluted into two. It can be noted that the dip in the intensity obtained after background subtraction is due to that the pure solvent and the sample with cellulose did not entirely match, indicating that the structure of the NaOH might change upon addition of cellulose. This might be supported by the results from the DSC measurements presented earlier in this thesis. There it was observed that upon addition of cellulose to NaOH(aq), there was a drastic decrease in the enthalpy of the NaOH hydrate and the melting point was slightly altered. However, background subtraction of the X-ray scattering did not alter the position of the cellulose peak, and the original data can be viewed in the supporting information for Paper IV.

For the 50/50 combination, two peaks could be identified, although they were weak (Figure 3.20b). The presence of diffraction peaks show that the cellulose can form a reoccurring structure despite the presence of two bases, but the weak signal shows that there is not much crystalline material in the sample.

In order to further investigate the intracrystalline swelling, the samples that were swollen at – 20 °C were also measured with solid-state NMR. The ^{13}C CP/MAS spectra can be seen in Figure 3.21. These measurements were in agreement with what was observed with X-ray diffraction, in that the spectra could not be assigned to either cellulose I or cellulose II. For the sample with MCC swelled in NaOH, the spectrum was similar to that obtained from wood pulp using similar treatments [107], and indicates a rather swollen structure. The spectrum of MCC swelled with TMAH showed several signals at relatively high order, however, although the pattern bears resemblance to that seen for cellulose II it was not this exact structure.

Upon coagulation of cellulose from a dissolved state, cellulose II is generally formed. This could possibly indicate that the relatively rapid aggregation of MCC in TMAH, seen in the stability measurements, is due to an order present already in the swollen state. The crystalline cellulose-TMAH complex (resembling cellulose II) could then act as a template for cellulose II formation, promoting aggregation. Noticeably, the MCC swelled with the 50/50 combination of NaOH and TMAH showed similar behaviour as the MCC swelled only with NaOH. This indicates that it is the NaOH rather than the TMAH that sets the structure in the 50/50 combination. However, the other results on the combination have reflected properties corresponding to an average of the two single-base solvents or synergistic properties. The results in general therefore indicate that both

bases influence the properties, but the ss-NMR shows that in the presence of both bases, the swollen cellulose does not form a crystalline complex similar to that which was observed with only TMAH. If the formation of a crystalline complex between TMAH and cellulose can explain the poor stability, a similar explanation can be proposed for the increased stability of the 50/50 combination. An analogy can be made between the effect that two bases closely interacting with the cellulose chains could have on crystallisation, and the detrimental effect that atacticity or irregular side groups can have on crystallisation of polymers. This could be important for the stability of the solutions if the presence of two bases does not provide a template for cellulose II formation.

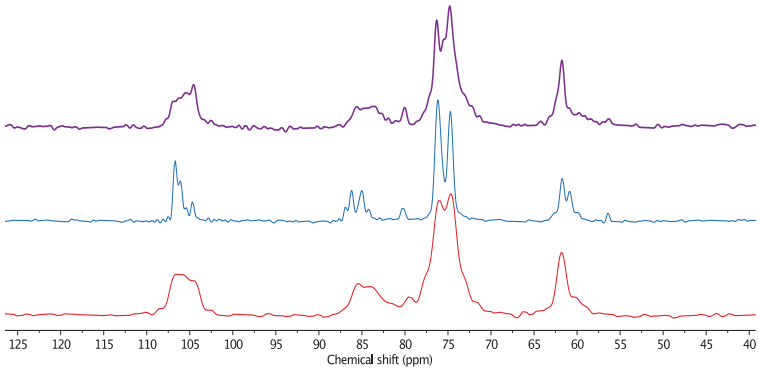

Figure 3.21: ^{13} CP/MAS NMR spectra of MCC swelled in NaOH(aq)(red), TMAH(aq)(blue), and 50/50 NaOH/TMAH(aq)(purple).

4 Summary and concluding remarks

The overarching objective of this thesis was to improve knowledge on aqueous hydroxide bases as solvents for cellulose. Since research on these solvents has been ongoing for almost 100 years, conducted both within academia and within industry, there is a lot of knowledge to build on. One reflection that can be made after investigating dissolution of cellulose, is that it is vital to remember that the properties of the solutions are highly dependent on several factors. This includes, but is not limited to, the base and type of cellulose chosen, the concentration of the base and of the cellulose, as well as the temperature applied both for dissolution and analysis. Because of this, measurements often do not reveal the entire picture at first, and it proves important to keep this in mind during interpretation of the results.

The fact that there are many forces at play in the solutions is good to remember when discussing the mechanism and driving forces behind dissolution. When cellulose is dissolved in aqueous hydroxide base solvents, surely almost all of the different types of intermolecular interactions could be accounted for. The solutions contain water (a hydrogen bonding polar liquid), cellulose (a polymer) and base (ions); together these molecules can create hydrogen bonds, accumulate numerous van der Waals interactions and most likely ion-to dipole and ion-induced dipole interactions. In the solid state, both hydrogen bonding and dispersion forces have been shown to play an important role, and upon dissolution other effects such as the hydrophobic assembly effect and deprotonation of the hydroxyl groups also need to be considered. Despite the difficulties in understanding how each and every interaction may contribute, some concluding remarks on the findings in this thesis can be made.

As evident through this work, the choice of hydroxide base affects the dissolution capacity, the temperature at which dissolution occurs and the stability of the solutions. NaOH in an aqueous solution makes a poor solvent, with incomplete dissolution of low DP cellulose already at dilute concentrations. The instability of the solutions over time and with increasing temperature was also shown. In contrast, the quaternary ammonium hydroxides were shown to have a higher dissolution capacity, increasing with increasing hydrophobicity of the investigated cations. The scattering measurements indicated aggregation to different extents in all solvents, but the cellulose was most well-dissolved in Triton B and probably in part molecularly dissolved. X-ray measurements indicated that the cellulose was stiffer in solutions of TMAH or Triton B, compared to solutions with NaOH. From the solvatochromic parameters measured, it was observed that the dissolution capacity of the single-base solvents increased with increasing hydrogen bond donor ability. This could possibly be attributed to the hydroxide ions being less hydrated when paired with a more hydrophobic base. Despite the striking inverse temperature dependency of these solutions, no sig-

nificant temperature dependency could be detected with the solvatochromic dyes. It was however shown, that for microcrystalline cellulose, freezing of the solutions is not a requirement, as reaching low temperatures is sufficient.

Regarding the effect of adding urea to the solutions, it further improved dissolution in NaOH and/or TMAH but did not have a significant effect on dissolution or solution properties in Triton B. This could indicate that for Triton B, the role of urea to weaken the hydrophobic effect by replacing water in the hydration shell of the pyranose ring was already fulfilled by Triton B. In contrast, there are reports that urea will increase the dissolution capacity of other quaternary ammonium hydroxides of comparable hydrophobicity [79], indicating that other factors also need to be considered.

This work has also shown that it is possible to combine two hydroxide bases in an aqueous solution to dissolve cellulose, and that this can have a similar effect on cellulose dissolution as an additive such as urea. From this work it also seems that the two bases need to be able to dissolve cellulose as a single base solvent, within the same temperature range, and be miscible with each other. Regarding the stability of the solutions, the hypothesis was that compared to NaOH, a more hydrophobic base would contribute to increased stability with increasing temperature. The findings revealed a different picture, where the combination of NaOH and TMAH improved stability and delayed aggregation not only compared to pure NaOH(aq), but also to pure TMAH(aq). Upon investigating the swollen state of cellulose, a more ordered crystalline complex was observed for cellulose in TMAH(aq), compared to NaOH(aq) or the combination. A tentative explanation, based on X-ray diffraction and solid-state NMR, was that if a more ordered complex can be formed between the cellulose and the base, this can act as a template for cellulose II and facilitate aggregation of the cellulose. In a similar manner, the presence of two bases might hinder the formation of a stable complex and therefore delay aggregation.

In its entirety, this work has built upon the existing knowledge of dissolution of cellulose in aqueous hydroxide bases, and expanded the knowledge on these solvents through modern techniques and by comparing and combining bases. Despite this, many questions remain and a few suggestions on future work are presented in the following section.

5 Future Work

For future work, it would be interesting to fully investigate the temperature dependency as a function of base concentration for bases that display two concentration regions at which they can dissolve cellulose. This could be correlated to properties such as basicity, hydrophobicity, hydrogen bonding ability, the presence of free water etc.

Further effort could also be made to validate the hypothesis that upon aggregation of cellulose from a dissolved state, there is a pre-stage to cellulose II crystallization that includes a complex between the cellulose and the base.

With regard to the combinations, it would be interesting to further investigate the potential of the NaOH/TMAH/urea(aq) solution, as a comparably high dissolution capacity was observed. However, due to the toxicity of TMAH, it is of importance to find a non-toxic quaternary ammonium hydroxide to replace it, keeping in mind the criteria for combining bases. What should also be properly addressed is the potential degradation of the quaternary ammonium hydroxides, even though the hypothesis is that the degradation is low when used at low temperatures and more dilute concentrations.

Regarding methodology, the models used for both analysis of light scattering and X-ray scattering are often not developed with highly polydisperse material like cellulose in mind. An effort could therefore be made to evaluate what analysis methods truly reflect the properties of the cellulose, or to create new models.

Bibliography

1. Nilsson, P., Roberge, C. & Fridman, J. Skogsdata 2021. ISSN: 0280-0543 (2021).
2. Föreningen Skogsindustrierna, ansvarig utgivare: Lisa Alexandersson. *Statistik om skog och industri* `https://www.skogsindustrierna.se/om-skogsindustrin/branschstatistik/` (2022).
3. Klemm, D., Heublein, B., Fink, H.-P. & Bohn, A. Cellulose: Fascinating Biopolymer and Sustainable Raw Material. *Angewandte Chemie International Edition* **44,** 3358–3393 (2005).
4. Berg, P. & Lingqvist, O. *Pulp, paper, and packaging in the next decade: Transformational change* tech. rep. (McKinsey Company, 2019).
5. Oberlerchner, J. T., Rosenau, T. & Potthast, A. Overview of Methods for the Direct Molar Mass Determination of Cellulose. *Molecules* **20,** 10313–10341 (2015).
6. Koso, T. *et al.* 2D Assignment and quantitative analysis of cellulose and oxidized celluloses using solution-state NMR spectroscopy. *Cellulose* **27,** 7929–7953 (2020).
7. Nishiyama, Y., Sugiyama, J., Chanzy, H. & Langan, P. Crystal Structure and Hydrogen Bonding System in Cellulose Iα from Synchrotron X-ray and Neutron Fiber Diffraction. *Journal of the American Chemical Society* **125,** 14300–14306 (2003).
8. Henriksson, G. & Lennholm, H. in *The Ljungberg Textbook* 57–85 (Fibre and Polymer Technology, KTH, Stockholm, 2011).
9. Nishiyama, Y. Molecular interactions in nanocellulose assembly. *Philosophical Transactions of the Royal Society A: Mathematical, Physical and Engineering Sciences* **376,** 20170047 (2018).
10. Wohlert, M. *et al.* Cellulose and the role of hydrogen bonds: not in charge of everything. *Cellulose* **29,** 1–23 (2022).
11. Gibson, L. J. The hierarchical structure and mechanics of plant materials. *Journal of The Royal Society Interface* **9,** 2749–2766 (2012).
12. Schmulsky, R. & Jones, D. in *Forest Products and Wood Science An Introduction* p. 45–63 (John Wiley Sons, Ltd). ISBN: 9780470960035.
13. Kolpak, F. J., Weih, M. & Blackwell, J. Mercerization of cellulose: 1. Determination of the structure of Mercerized cotton. *Polymer* **19,** 123–131 (1978).
14. Sèbe, G., Ham-Pichavant, F., Ibarboure, E., Koffi, A. L. C. & Tingaut, P. Supramolecular Structure Characterization of Cellulose II Nanowhiskers Produced by Acid Hydrolysis of Cellulose I Substrates. *Biomacromolecules* **13,** 570–578 (2012).

15. Ago, M., Endo, T. & Hirotsu, T. Crystalline transformation of native cellulose from cellulose I to cellulose ID polymorph by a ball-milling method with a specific amount of water. *Cellulose* **11,** 163–167 (2004).

16. Kroon-Batenburg, L. M. J. & Kroon, J. The crystal and molecular structures of cellulose I and II. *Glycoconjugate Journal* **14,** 677–690 (1997).

17. Langan, P., Nishiyama, Y. & Chanzy, H. A Revised Structure and Hydrogen-Bonding System in Cellulose II from a Neutron Fiber Diffraction Analysis. *Journal of the American Chemical Society* **121,** 9940–9946 (1999).

18. Gedde, U. W. in *Polymer Physics* p. 55–75 (Springer Netherlands, Dordrecht, 1999). ISBN: 978-94-011-0543-9.

19. Rathee, V. S., Sidky, H., Sikora, B. J. & Whitmer, J. K. Role of Associative Charging in the Entropy–Energy Balance of Polyelectrolyte Complexes. *Journal of the American Chemical Society* **140,** 15319–15328 (2018).

20. Rubinstein Michael, C. R. H. in *Polymer Physics* p. 49–96 (Oxford University Press, 2003). ISBN: 978-0-19-852059-7.

21. Milstein, J. N. & Meiners, J.-C. in *Encyclopedia of Biophysics* p. 2757–2760 (Springer Berlin Heidelberg, Berlin, Heidelberg, 2013). ISBN: 978-3-642-16712-6.

22. Miller-Chou, B. A. & Koenig, J. L. A review of polymer dissolution. *Progress in Polymer Science* **28,** 1223–1270 (2003).

23. Le Moigne, N., Spinu, M., Heinze, T. & Navard, P. Restricted dissolution and derivatization capacities of cellulose fibres under uniaxial elongational stress. *Polymer* **51,** 447–453 (2010).

24. Lindman, B., Karlström, G. & Stigsson, L. On the mechanism of dissolution of cellulose. *Journal of Molecular Liquids* **156,** 76–81 (2010).

25. Chandler, D. Interfaces and the driving force of hydrophobic assembly. *Nature* **437,** 640–647 (2005).

26. Moigne, N. & Navard, P. Dissolution mechanisms of wood cellulose fibres in NaOH–water. *Cellulose* **17,** 31–45 (2010).

27. Le Moigne, N., Montes, E., Pannetier, C., Höfte, H. & Navard, P. Gradient in Dissolution Capacity of Successively Deposited Cell Wall Layers in Cotton Fibres. *Macromolecular Symposia* **262,** 65–71 (2008).

28. Budtova, T. & Navard, P. Cellulose in NaOH–water based solvents: a review. *Cellulose* **23,** 5–55 (2016).

29. Davidson, G. F. The dissolution of chemically modified cotton cellulose in alkaline solutions. Part I - In solutions of sodium hydroxide, particularly at temperatures below the normal. *Journal of the Textile Institute Transactions* **25,** T174–T196 (1934).

30. Magnusson, H. *From recovery boiler to integration of a textile fiber plant: Combination of mass balance analysis and chemical engineering* PhD thesis (Karlstads universitet, 2015).

31. Harlin, A. *Cellulose carbamate: production and applications* English (VTT Technical Research Centre of Finland, Finland, 2019).

32. Swatloski, R. P., Spear, S. K., Holbrey, J. D. & Rogers, R. D. Dissolution of Cellose with Ionic Liquids. *Journal of the American Chemical Society* **124,** 4974–4975 (2002).

33. Wang, H., Gurau, G. & Rogers, R. D. Ionic liquid processing of cellulose. *Chemical Society Reviews* **41,** 1519–1537 (2012).

34. Heinze, T. *et al.* Interactions of Ionic Liquids with Polysaccharides – 2: Cellulose. *Macromolecular Symposia* **262,** 8–22 (2008).

35. McCormick, C. L., Callais, P. A. & Hutchinson, B. H. Solution studies of cellulose in lithium chloride and N,N-dimethylacetamide. *Macromolecules* **18,** 2394–2401 (1985).

36. Rosenau, T., Potthast, A., Sixta, H. & Kosma, P. The chemistry of side reactions and byproduct formation in the system NMMO/cellulose (Lyocell process). *Progress in Polymer Science* **26,** 1763–1837 (2001).

37. Köhler, S. & Heinze, T. New Solvents for Cellulose: Dimethyl Sulfoxide/Ammonium Fluorides. *Macromolecular Bioscience* **7,** 307–314 (2007).

38. Cai, J. & Zhang, L. Rapid Dissolution of Cellulose in LiOH/Urea and NaOH/Urea Aqueous Solutions. *Macromolecular Bioscience* **5,** 539–548 (2005).

39. Fink, H.-P., Weigel, P., Purz, H. J. & Ganster, J. Structure formation of regenerated cellulose materials from NMMO-solutions. *Progress in Polymer Science* **26,** 1473–1524 (2001).

40. Rosenau, T. & French, A. D. N-Methylmorpholine-N-oxide (NMMO): hazards in practice and pitfalls in theory. *Cellulose* **28,** 5985–5990 (2021).

41. Davidson, G. F. 10-The dissolution of chemically modified cotton cellulose in alkaline solutions. Part II. A comparison of the solvent action of solutions of lithium, sodium, potassium, and tetramethylammonium hydroxides. *Journal of the Textile Institute Transactions* **27,** T112–T130 (1936).

42. Kostag, M., Jedvert, K., Achtel, C., Heinze, T. & El Seoud, O. A. Recent Advances in Solvents for the Dissolution, Shaping and Derivatization of Cellulose: Quaternary Ammonium Electrolytes and their Solutions in Water and Molecular Solvents. *Molecules* **23** (2018).

43. Zhong, C., Wang, C., Huang, F., Jia, H. & Wei, P. Wheat straw cellulose dissolution and isolation by tetra-n-butylammonium hydroxide. *Carbohydrate Polymers* **94,** 38–45 (2013).

44. Miao, J., Sun, H., Yu, Y., Song, X. & Zhang, L. Quaternary ammonium acetate: an efficient ionic liquid for the dissolution and regeneration of cellulose. *RSC Advances* **4,** 36721–36724 (2014).

45. Lilienfeld, L. US patent 1,658,606 (1928).

46. Sobue, H., Heinz, K. & Kurt, H. Das System Cellulose–Natriumhydroxyd–Wasser in Abhängigkeit von der Temperatur. *Zeitschrift für Physikalische Chemie* **43B,** 309 (1939).

47. Xiong, B. *et al.* NMR spectroscopic studies on the mechanism of cellulose dissolution in alkali solutions. *Cellulose* **20,** 613–621 (2013).

48. Lindman, B. *et al.* The relevance of structural features of cellulose and its interactions to dissolution, regeneration, gelation and plasticization phenomena. *Phys. Chem. Chem. Phys.* **19,** 23704–23718 (2017).

49. Isogai, A. NMR analysis of cellulose dissolved in aqueous NaOH solutions. *Cellulose* **4,** 99–107 (1997).

50. Bialik, E. *et al.* Ionization of Cellobiose in Aqueous Alkali and the Mechanism of Cellulose Dissolution. *The Journal of Physical Chemistry Letters* **7,** 5044–5048 (2016).

51. Malmsten, M. & Lindman, B. Ellipsometry studies of the adsorption of cellulose ethers. *Langmuir* **6,** 357–364 (Feb. 1990).

52. Bergenstråhle-Wohlert, M., Angles d'Ortoli, T., Sjöberg, N. A., Widmalm, G. & Wohlert, J. On the anomalous temperature dependence of cellulose aqueous solubility. *Cellulose* **23,** 2375–2387 (2016).

53. Gunnarsson, M., Hasani, M. & Bernin, D. Influence of urea on methyl β-D-glucopyranoside in alkali at different temperatures. *Cellulose* **26,** 9413–9422 (2019).

54. Yamashiki, T. *et al.* Some Characteristic Features of Dilute Aqueous Alkali Solutions of Specific Alkali Concentration (2.5 mol l-1) Which Possess Maximum Solubility Power against Cellulose. *Polym J* **20,** 447–457 (1988).

55. Roy, C., Budtova, T. & Navard, P. Rheological Properties and Gelation of Aqueous CelluloseNaOH Solutions. *Biomacromolecules* **4,** 259–264 (2003).

56. Hagman, J. *et al.* On the dissolution state of cellulose in cold alkali solutions. *Cellulose* **24,** 2003–2015 (2017).

57. Pereira, A. *et al.* Cellulose gelation in NaOH solutions is due to cellulose crystallization. *Cellulose* **25,** 3205–3210 (2018).

58. Isogai, A. & Atalla, R. H. Dissolution of Cellulose in Aqueous NaOH Solutions. *Cellulose* **5,** 309–319 (1998).

59. Wang, S. *et al.* Influence of cation on the cellulose dissolution investigated by MD simulation and experiments. *Cellulose* **24** (2017).

60. Lovell, C. S. *et al.* Influence of Cellulose on Ion Diffusivity in 1-Ethyl-3-Methyl-Imidazolium Acetate Cellulose Solutions. *Biomacromolecules* **11,** 2927–2935 (2010).

61. Wang, Y. & Deng, Y. The kinetics of cellulose dissolution in sodium hydroxide solution at low temperatures. *Biotechnology and Bioengineering* **102,** 1398–1405 (2009).

62. Lilienfeld, L. GB patent 217,166 (1924).

63. Powers, D. H. & Bock, L. H. US patent 2,009,015 (1935).

64. Brownsett, T. & Clibbens, D. A. 4—The dissolution of chemically modified cotton cellulose in alkaline solutions. Part VII. The solvent action of solutions of trimethylbenzyl-and dimethyldibenzyl-ammonium hydroxides (tritons B and F). *Journal of the Textile Institute Transactions* **32,** T32–T44 (1941).

65. Sisson, W. A. & Saner, W. R. An X-ray Diffraction Study of the Swelling Action of Several Quaternary Ammonium Hydroxides on Cellulose Fibers. *The Journal of Physical Chemistry* **43,** 687–699 (1939).

66. Wang, Y., Liu, L., Chen, P., Zhang, L. & Lu, A. Cationic hydrophobicity promotes dissolution of cellulose in aqueous basic solution by freezing–thawing. *Physical Chemistry Chemical Physics* **20,** 14223–14233 (2018).

67. Zhong, C. *et al.* Dissolution mechanism of cellulose in quaternary ammonium hydroxide: Revisiting through molecular interactions. *Carbohydrate Polymers* **174,** 400–408 (2017).

68. Gubitosi, M., Duarte, H., Gentile, L., Olsson, U. & Medronho, B. On cellulose dissolution and aggregation in aqueous tetrabutylammonium hydroxide. *Biomacromolecules* **17,** 2873–2881 (2016).

69. Abe, M., Fukaya, Y. & Ohno, H. Fast and facile dissolution of cellulose with tetrabutylphosphonium hydroxide containing 40 wt% water. *Chem. Commun.* **48,** 1808–1810 (2012).

70. Abe, M., Kuroda, K. & Ohno, H. Maintenance-Free Cellulose Solvents Based on Onium Hydroxides. *ACS Sustainable Chemistry Engineering* **3,** 1771–1776 (2015).

71. Hyväkkö, U., King, A. & Kilpeläinen, I. Extraction of Wheat Straw with Aqueous Tetra-n-Butylphosphonium Hydroxide. *BioResources* **9** (2014).

72. Davidson, G. F. 4.—The dissolution of chemically modified cotton cellulose in alkaline solutions. Part 3—in solutions of sodium and potassium hydroxide containing dissolved zinc, beryllium and aluminium oxides. *Journal of the Textile Institute Transactions* **28,** T27–T44 (1937).

73. Yang, Q. *et al.* Role of sodium zincate on cellulose dissolution in NaOH/urea aqueous solution at low temperature. *Carbohydrate Polymers* **83,** 1185–1191 (2011).

74. Jiang, Z. *et al.* Dissolution and Metastable Solution of Cellulose in NaOH/ Thiourea at 8 °C for Construction of Nanofibers. *The Journal of Physical Chemistry B* **121,** 1793–1801 (2017).

75. Yan, L. & Gao, Z. Dissolving of cellulose in PEG/NaOH aqueous solution. *Cellulose* **15,** 789–796 (2008).

76. Liu, W., Budtova, T. & Navard, P. Influence of ZnO on the properties of dilute and semi-dilute cellulose-NaOH-water solutions. *Cellulose* **18,** 911–920 (2011).

77. Cai, J. & Zhang, L. Unique Gelation Behavior of Cellulose in NaOH/Urea Aqueous Solution. *Biomacromolecules* **7,** 183–189 (2006).

78. Zhang, S., Li, F.-X., Yu, J.-y. & Hsieh, Y.-L. Dissolution behaviour and solubility of cellulose in NaOH complex solution. *Carbohydrate Polymers* **81,** 668–674 (2010).

79. Sirviö, J. A. & Heiskanen, J. P. Room-temperature dissolution and chemical modification of cellulose in aqueous tetraethylammonium hydroxide– carbamide solutions. *Cellulose* **27,** 1933–1950 (2019).

80. Grönqvist, S. *et al.* Enhanced pre-treatment of cellulose pulp prior to dissolution into NaOH/ZnO. *Cellulose* **22,** 3981–3990 (2015).

81. Engström, J. WO2020231315A1 (2020).

82. IFF/DuPont. *Avicel* `https://www.pharma.dupont.com/pharmaceutical-brands/avicelr-for-solid-dose-forms.html`.

83. Swensson, B., Larsson, A. & Hasani, M. Dissolution of cellulose using a combination of hydroxide bases in aqueous solution. *Cellulose* **27,** 101–112 (2020).

84. Swensson, B., Larsson, A. & Hasani, M. Probing Interactions in Combined Hydroxide Base Solvents for Improving Dissolution of Cellulose. *Polymers* **12,** 1310 (2020).

85. Seiler, E. R. D., Takeoka, Y., Rikukawa, M. & Yoshizawa-Fujita, M. Development of a novel cellulose solvent based on pyrrolidinium hydroxide and reliable solubility analysis. *RSC Adv.* **10,** 11475–11480 (2020).

86. Ab Rani, M. A. *et al.* Understanding the polarity of ionic liquids. *Phys. Chem. Chem. Phys.* **13,** 16831–16840 (2011).

87. Kamlet, M. J., Abboud, J. L. & Taft, R. W. The solvatochromic comparison method. 6. The .pi.* scale of solvent polarities. *Journal of the American Chemical Society* **99,** 6027–6038 (1977).

88. Kamlet, M. J. & Taft, R. W. The solvatochromic comparison method. I. The .beta.-scale of solvent hydrogen-bond acceptor (HBA) basicities. *Journal of the American Chemical Society* **98,** 377–383 (1976).

89. Taft, R. W. & Kamlet, M. J. The solvatochromic comparison method. 2. The .alpha.-scale of solvent hydrogen-bond donor (HBD) acidities. *Journal of the American Chemical Society* **98,** 2886–2894 (1976).

90. Lee, C.-Y., McCammon, J. A. & Rossky, P. J. The structure of liquid water at an extended hydrophobic surface. *The Journal of Chemical Physics* **80,** 4448–4455 (1984).

91. Pires, P. A. R. *et al.* Understanding Solvation: Comparison of Reichardt's Solvatochromic Probe and Related Molecular "Core" Structures. *Journal of Chemical Engineering Data* **64,** 2213–2220 (2019).

92. Swensson, B., Lages, S., Berke, B., Larsson, A. & Hasani, M. Scattering studies of the size and structure of cellulose dissolved in aqueous hydroxide base solvents. *Carbohydrate Polymers* **274,** 118634 (2021).

93. Attwood, D. & Florence, A. in. Second edi, p. 54 (2012). ISBN: 9780857110640.

94. Lu, A., Liu, Y., Zhang, L. & Potthast, A. Investigation on Metastable Solution of Cellulose Dissolved in NaOH/Urea Aqueous System at Low Temperature. *The Journal of Physical Chemistry B* **115,** 12801–12808 (2011).

95. Glatter, O. in *Scattering Methods and their Application in Colloid and Interface Science* p. 33–74 (Elsevier, 2018). ISBN: 978-0-12-813580-8.

96. Pedersen, J. S. & Schurtenberger, P. Scattering Functions of Semiflexible Polymers with and without Excluded Volume Effects. *Macromolecules* **29,** 7602–7612 (1996).

97. Schulz, L., Seger, B. & Burchard, W. Structures of cellulose in solution. *Macromolecular Chemistry and Physics* **201,** 2008–2022 (2000).

98. Costa, C. *et al.* Lignin enhances cellulose dissolution in cold alkali. *Carbohydrate Polymers* **274,** 118661 (2021).

99. Roy, C., Budtova, T., Navard, P. & Bedue, O. Structure of CelluloseSoda Solutions at Low Temperatures. *Biomacromolecules* **2,** 687–693 (2001).

100. Mootz, D. & Seidel, R. Polyhedral clathrate hydrates of a strong base: Phase relations and crystal structures in the system tetramethylammonium hydroxide-water. *Journal of inclusion phenomena and molecular recognition in chemistry* **8,** 139–157 (1990).

101. Pickering, S. U. LXI.—The hydrates of sodium, potassium, and lithium hydroxides. *J. Chem. Soc., Trans.* **63,** 890–909 (1893).

102. Egal, M., Budtova, T. & Navard, P. Structure of Aqueous Solutions of Microcrystalline Cellulose/Sodium Hydroxide below 0 °C and the Limit of Cellulose Dissolution. *Biomacromolecules* **8,** 2282–2287 (2007).

103. Sippola, H. & Taskinen, P. Activity of Supercooled Water on the Ice Curve and Other Thermodynamic Properties of Liquid Water up to the Boiling Point at Standard Pressure. *Journal of Chemical Engineering Data* **63,** 2986–2998 (2018).

104. Alfredsson, B. & Sauelson, O. Hydroxy acids formed by alkali treatment of hydrocellulose. *Svensk Papperstidning,* 679–686 (1968).

105. Li, W. *et al.* Fivefold Helical Cellulose Trapped in a Sulfuric Acid Framework. *Crystal Growth Design* **22,** 20–25 (2022).

106. Nam, S., French, A. D., Condon, B. D. & Concha, M. Segal crystallinity index revisited by the simulation of X-ray diffraction patterns of cotton cellulose Iβ and cellulose II. *Carbohydrate Polymers* **135,** 1–9 (2016).

107. Porro, F., Bédué, O., Chanzy, H. & Heux, L. Solid-State 13C NMR Study of NaCellulose Complexes. *Biomacromolecules* **8,** 2586–2593 (2007).